

Physics potential of the CERN-MEMPHYS neutrino oscillation project

Jean-Eric Campagne,^a Michele Maltoni,^b Mauro Mezzetto^c and Thomas Schwetz^d

^aLaboratoire de l'Accélérateur Linéaire, Université Paris-Sud
IN2P3/CNRS, B.P. 34, 91898 Orsay Cedex, France

^bInternational Centre for Theoretical Physics,
Strada Costiera 11, I-31014 Trieste, Italy, and
Departamento de Física Teórica and Instituto de Física Teórica
Facultad de Ciencias C-XI, Universidad Autónoma de Madrid,
Cantoblanco, E-28049 Madrid, Spain

^cIstituto Nazionale Fisica Nucleare, Sezione di Padova
via Marzolo 8, 35100 Padova, Italy

^dScuola Internazionale Superiore di Studi Avanzati
via Beirut 2-4, 34014 Trieste, Italy, and
CERN, Physics Department, Theory Division,
CH-1211 Geneva 23, Switzerland
E-mail: campagne@lal.in2p3.fr, michele.maltoni@uam.es,
mauro.mezzetto@pd.infn.it, schwetz@cern.ch

ABSTRACT: We consider the physics potential of CERN based neutrino oscillation experiments consisting of a Beta Beam (βB) and a Super Beam (SPL) sending neutrinos to MEMPHYS, a 440 kt water Čerenkov detector at Fréjus, at a distance of 130 km from CERN. The θ_{13} discovery reach and the sensitivity to CP violation are investigated, including a detailed discussion of parameter degeneracies and systematical errors. For SPL sensitivities similar to the ones of the phase II of the T2K experiment (T2HK) are obtained, whereas the βB may reach significantly better sensitivities, depending on the achieved number of total ion decays. The results for the CERN-MEMPHYS experiments are less affected by systematical uncertainties than T2HK. We point out that by a combination of data from βB and SPL a measurement with antineutrinos is not necessary and hence the same physics results can be obtained within about half of the measurement time compared to one single experiment. Furthermore, it is shown how including data from atmospheric neutrinos in the MEMPHYS detector allows to resolve parameter degeneracies and, in particular, provides sensitivity to the neutrino mass hierarchy and the octant of θ_{23} .

KEYWORDS: Neutrino Physics, Solar and Atmospheric Neutrinos.

Contents

1. Introduction	1
2. Experiments overview and analysis methods	3
3. The CERN-MEMPHYS experiments	5
3.1 The MEMPHYS detector	5
3.2 The $\gamma = 100 \times 100$ baseline Beta Beam	5
3.3 The 3.5-GeV SPL Super Beam	8
3.4 The atmospheric neutrino analysis	10
4. Degeneracies	12
5. Physics potential	16
5.1 Sensitivity to the atmospheric parameters	16
5.2 The θ_{13} discovery potential	17
5.3 Sensitivity to CP violation	20
6. Synergies provided by the CERN-MEMPHYS facilities	24
6.1 Combining Beta Beam and Super Beam	24
6.2 Resolving degeneracies with atmospheric neutrinos	25
7. Summary	28

1. Introduction

In recent years strong evidence for neutrino oscillations has been obtained in solar [1], atmospheric [2, 3], reactor [4], and accelerator [5] neutrino experiments. The very near future of long-baseline (LBL) neutrino experiments is devoted to the study of the oscillation mechanism in the range of $\Delta m_{31}^2 \approx 2.4 \times 10^{-3} \text{ eV}^2$ indicated by atmospheric neutrinos using conventional ν_μ beams. Similar as in the K2K experiment in Japan [5], the presently running MINOS experiment in the USA [6] uses a low energy beam to measure Δm_{31}^2 by observing the $\nu_\mu \rightarrow \nu_\mu$ disappearance probability, while the OPERA [7] experiment will be able to detect ν_τ appearance within the high energy CERN-Gran Sasso beam [8]. If we do not consider the LSND anomaly [9] that will be further studied soon by the MiniBooNE experiment [10], all data can be accommodated within the three flavor scenario (see refs. [11, 12] for recent global analyses), and neutrino oscillations are described by two

neutrino mass-squared differences (Δm_{21}^2 and Δm_{31}^2) and the 3×3 unitary Pontecorvo-Maki-Nakagawa-Sakata (PMNS) lepton mixing matrix [13] with three angles ($\theta_{12}, \theta_{13}, \theta_{23}$) and one Dirac CP phase δ_{CP} .

Future tasks of neutrino physics are an improved sensitivity to the last unknown mixing angle, θ_{13} , to explore the CP violation mechanism in the leptonic sector, and to determine the sign of Δm_{31}^2 which describes the type of the neutrino mass hierarchy (normal, $\Delta m_{31}^2 > 0$ or inverted, $\Delta m_{31}^2 < 0$). The present upper bound on θ_{13} is dominated by the constraint from the Chooz reactor experiment [14]. A global analysis of all data yields $\sin^2 2\theta_{13} < 0.082$ at 90% CL [12]. A main purpose of upcoming reactor and accelerator experiments is to improve this bound or to reveal a finite value of θ_{13} . In reactor experiments, one uses $\bar{\nu}_e$ in disappearance mode and the sensitivity is increased with respect to present experiments by the use of a near detector close to the reactor [15]. In accelerator experiments, the first generation of so-called Super Beams with sub-mega watt proton drivers such as T2K (phase-I) [16] and NO ν A [17], the appearance channel $\nu_\mu \rightarrow \nu_e$ is explored. This next generation of reactor and Super Beam experiments will reach sensitivities of the order of $\sin^2 2\theta_{13} \lesssim 0.01$ (90% CL) within a time scale of several years [18]. Beyond this medium term program, there are several projects on how to enter the high precision age in neutrino oscillations and to attack the ultimate goals like the discovery of leptonic CP violation or the determination of the neutrino mass hierarchy. In accelerator experiments, one can extend the Super Beam concept by moving to multi-mega watt proton drivers [16, 19–21] or apply novel technologies, such as neutrino beams from decaying ions (so-called Beta Beams) [22, 23] or from decaying muons (so-called Neutrino Factories) [23, 24].

In this work we focus on possible future neutrino oscillation facilities hosted at CERN, namely a multi-mega watt Super Beam experiment based on a Super Proton Linac (SPL) [25] and a $\gamma = 100$ Beta Beam (βB) [26]. These experiments will search for $(\bar{\nu})_\mu \rightarrow (\bar{\nu})_e$ and $(\bar{\nu})_e \rightarrow (\bar{\nu})_\mu$ appearance, respectively, by sending the neutrinos to a mega ton scale water Čerenkov detector (MEMPHYS) [27], located at a distance of 130 km from CERN under the Fréjus mountain. Similar detectors are under consideration also in the US (UNO [28]) and in Japan (Hyper-K [16, 29]). We perform a detailed analysis of the SPL and βB physics potential, discussing the discovery reach for θ_{13} and leptonic CP violation. In addition we consider the possibility to resolve parameter degeneracies in the LBL data by using the atmospheric neutrinos available in the mega ton detector [30]. This leads to a sensitivity to the neutrino mass hierarchy of the CERN-MEMPHYS experiments, despite the rather short baseline. The physics performances of βB and SPL are compared to the ones obtainable at the second phase of the T2K experiment in Japan, which is based on an upgraded version of the original T2K beam and the Hyper-K detector (T2HK) [16].

The outline of the paper is as follows. In section 2 we summarize the main characteristics of the βB , SPL, and T2HK experiments and give general details of the physics analysis methods, whereas in section 3 we describe in some detail the MEMPHYS detector, the βB , the SPL Super Beam, and our atmospheric neutrino analysis. In section 4 we review the problem of parameter degeneracies and discuss its implications for the experiments under consideration. In section 5 we present the sensitivities to the “atmospheric parameters”

	β B	SPL	T2HK
Detector mass	440 kt	440 kt	440 kt
Baseline	130 km	130 km	295 km
Running time ($\nu + \bar{\nu}$)	5 + 5 yr	2 + 8 yr	2 + 8 yr
Beam intensity	$5.8 (2.2) \cdot 10^{18}$ He (Ne) dcys/yr	4 MW	4 MW
Systematics on signal	2%	2%	2%
Systematics on backgr.	2%	2%	2%

Table 1: Summary of default parameters used for the simulation of the β B, SPL, and T2HK experiments.

θ_{23} and Δm_{31}^2 , the θ_{13} discovery potential, and the sensitivity to CP violation. We also investigate in some detail the impact of systematical errors. In section 6 we discuss synergies which are offered by the CERN-MEMPHYS facilities. We point out advantages of the case when β B and SPL are available simultaneously, and we consider the use of atmospheric neutrino data in MEMPHYS in combination with the LBL experiments. Our results are summarized in section 7.

2. Experiments overview and analysis methods

In this section we give the most important experimental parameters which we adopt for the simulation of the CERN-MEMPHYS experiments β B and SPL, as well as for the T2HK experiment in Japan. These parameters are summarized in table 1. For all experiments the detector mass is 440 kt, and the running time is 10 years, with a division in neutrino and antineutrino running time in such a way that roughly an equal number of events is obtained. We always use the total available information from appearance as well as disappearance channels including the energy spectrum. For all three experiments we adopt rather optimistic values for the systematical uncertainties of 2% as default values, but we also consider the case when systematics are increased to 5%. These errors are uncorrelated between the various signal channels (neutrinos and antineutrinos), and between signals and backgrounds.

A more detailed description of the CERN-MEMPHYS experiments is given in section 3. For the T2HK simulation we use the setup provided by GLoBES [31] based on ref. [32], which follows closely the LOI [16]. In order to allow a fair comparison we introduce the following changes with respect to the configuration used in ref. [32]: The fiducial mass is set to 440 kt, the systematical errors on the background and on the ν_e and $\bar{\nu}_e$ appearance signals is set to 2%, and we use a total running time of 10 years, divided into 2 years of data taking with neutrinos and 8 years with antineutrinos. We include an additional background from the $\bar{\nu}_\mu \rightarrow \bar{\nu}_e$ ($\nu_\mu \rightarrow \nu_e$) channel in the neutrino (antineutrino) mode. Furthermore, we use the same CC detection cross section as for the β B/SPL analysis [33]. For more details see refs. [16, 32].

Recently the idea was put forward to observe the T2K beam with a second detector placed in Korea [34–36]. In the so-called T2KK setup the Hyper-Kamiokande detector is

	βB		SPL		T2HK	
	$\delta_{\text{CP}} = 0$	$\delta_{\text{CP}} = \pi/2$	$\delta_{\text{CP}} = 0$	$\delta_{\text{CP}} = \pi/2$	$\delta_{\text{CP}} = 0$	$\delta_{\text{CP}} = \pi/2$
appearance ν						
background	143		622		898	
$\sin^2 2\theta_{13} = 0$	28		51		83	
$\sin^2 2\theta_{13} = 10^{-3}$	76	88	105	14	178	17
$\sin^2 2\theta_{13} = 10^{-2}$	326	365	423	137	746	238
appearance $\bar{\nu}$						
background	157		640		1510	
$\sin^2 2\theta_{13} = 0$	31		57		93	
$\sin^2 2\theta_{13} = 10^{-3}$	83	12	102	146	192	269
$\sin^2 2\theta_{13} = 10^{-2}$	351	126	376	516	762	1007
disapp. ν						
background	100315		21653		24949	
disapp. $\bar{\nu}$	6		1		444	
disapp. $\bar{\nu}$						
background	84125		18321		34650	
background	5		1		725	

Table 2: Number of events for appearance and disappearance signals and backgrounds for the βB , SPL, and T2HK experiments as defined in table 1. For the appearance signals the event numbers are given for several values of $\sin^2 2\theta_{13}$ and $\delta_{\text{CP}} = 0$ and $\pi/2$. The background as well as the disappearance event numbers correspond to $\theta_{13} = 0$. For the other oscillation parameters the values of eq. (2.1) are used.

split into two detectors of 270 kt each, one of them is located in Korea at a distance of about 1050 km from the source, and the other is placed at Kamioka at a distance of 295 km. Here we will confine ourselves to the standard T2HK setup, since the purpose of our work is not a T2HK optimization study investigating various configurations for that experiment. In contrast, here T2HK mainly serves as a point of reference to which we compare the CERN-MEMPHYS experiments. For this aim we prefer to stick to the “minimal” one-detector configuration at a relatively short baseline, since two-detector setups with very long baselines clearly represent a different class of experiments whose consideration goes beyond the scope of the present work. Nevertheless we will comment briefly also on T2KK performances obtained in refs. [34, 35].

In table 2 we give the number of signal and background events for the experiment setups as defined in table 1. For the appearance channels ($\bar{\nu}_e \rightarrow \bar{\nu}_\mu$ for the βB and $\bar{\nu}_\mu \rightarrow \bar{\nu}_e$ for SPL and T2HK) we give the signal events for various values of θ_{13} and δ_{CP} . The “signal” events for $\theta_{13} = 0$ are appearance events induced by the oscillations with Δm_{21}^2 . The value $\sin^2 2\theta_{13} = 10^{-3}$ corresponds roughly to the sensitivity limit for the considered experiments, whereas $\sin^2 2\theta_{13} = 10^{-2}$ gives a good sensitivity to CP violation. This can be appreciated by comparing the values of ν and $\bar{\nu}$ appearance events for $\delta_{\text{CP}} = 0$ and $\pi/2$. In the table the background to the appearance signal is given for $\theta_{13} = 0$. Note that in general the number of background events depends also on the oscillation parameters, since also the background neutrinos in the beam oscillate. This effect is consistently taken into

account in the analysis, however, for the parameter values in the table the change in the background events due to oscillations is only of the order of a few events.

The physics analysis is performed with the GLOBES open source software [31], which provides a convenient tool to simulate long-baseline experiments and compare different facilities in a unified framework. The experiment definition (AEDL) files for the β B and SPL simulation with GLOBES are available at ref. [31]. In the analysis parameter degeneracies and correlations are fully taken into account and in general all oscillation parameters are varied in the fit. To simulate the “data” we adopt the following set of “true values” for the oscillation parameters:

$$\begin{aligned} \Delta m_{31}^2 &= +2.4 \times 10^{-3} \text{ eV}^2, & \sin^2 \theta_{23} &= 0.5, \\ \Delta m_{21}^2 &= 7.9 \times 10^{-5} \text{ eV}^2, & \sin^2 \theta_{12} &= 0.3, \end{aligned} \tag{2.1}$$

and we include a prior knowledge of these values with an accuracy of 10% for θ_{12} , θ_{23} , Δm_{31}^2 , and 4% for Δm_{21}^2 at 1σ . These values and accuracies are motivated by recent global fits to neutrino oscillation data [11, 12], and they are always used except where explicitly stated otherwise.

3. The CERN-MEMPHYS experiments

3.1 The MEMPHYS detector

MEMPHYS (MEgaton Mass PHYSics) [27] is a mega ton class water Čerenkov detector in the straight extrapolation of Super-Kamiokande, located at Fréjus, at a distance of 130 km from CERN. It is an alternative design of the UNO [28] and Hyper-Kamiokande [29] detectors and shares the same physics case, both from the non-accelerator domain (nucleon decay, super nova neutrino detection, solar neutrinos, atmospheric neutrinos) and from the accelerator domain which is the subject of this paper. A recent civil engineering pre-study to envisage the possibly of large cavity excavation located under the Fréjus mountain (4800 m.e.w.) near the present Modane underground laboratory has been undertaken. The main result of this pre-study is that MEMPHYS may be built with present techniques as a modular detector consisting of several shafts, each with 65 m in diameter, 65 m in height for the total water containment. A schematic view of the layout is shown in figure 1. For the present study we have chosen a fiducial mass of 440 kt which means 3 shafts and an inner detector of 57 m in diameter and 57 m in height. Each inner detector may be equipped with photo detectors (81000 per shaft) with a 30% geometrical coverage and the same photo-statistics as Super-Kamiokande (with a 40% coverage). In principle up to 5 shafts are possible, corresponding to a fiducial mass of 730 kt. The Fréjus site offers a natural protection against cosmic rays by a factor 10^6 . If not mentioned otherwise, the event selection and particle identification are the Super-Kamiokande algorithms results.

3.2 The $\gamma = 100 \times 100$ baseline Beta Beam

The concept of a Beta Beam (β B) has been introduced by P. Zucchelli in ref. [22]. Neutrinos are produced by the decay of radioactive isotopes which are stored in a decay ring. An

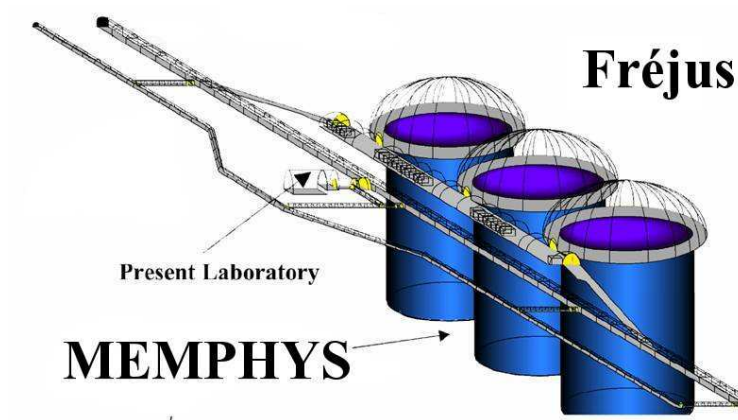


Figure 1: Sketch of the MEMPHYS detector under the Fréjus mountain.

important parameter is the relativistic gamma factor of the ions, which determines the energy of the emitted neutrinos. β B performances have been computed previously for $\gamma(^6\text{He}) = 66$ [26], 100 [37–39], 150 [39], 200 [40], 350 [39], 500 [41, 40], 1000 [40], 2000 [41], 2488 [42]. Reviews can be found in ref. [43], the physics potential of a very low gamma β B has been studied in ref. [44]. Performances of a β B with $\gamma > 150$ are extremely promising, however, they are neither based on an existing accelerator complex nor on detailed calculations of the ion decay rates. For a CERN based β B, fluxes have been estimated in ref. [45] and a design study is in progress for the facility [46]. In this work we assume an integrated flux of neutrinos in 10 years corresponding to $2.9 \cdot 10^{19}$ useful ^6He decays and $1.1 \cdot 10^{19}$ useful ^{18}Ne decays. These fluxes have been assumed in all the physics papers quoted above, and they are two times higher than the baseline fluxes computed in ref. [45]. These latter fluxes suffer for the known limitations of the PS and SPS synchrotrons at CERN, ways to improve them have been delineated in ref. [48].

The infrastructure available at CERN as well as the MEMPHYS location at a distance of 130 km suggest a γ -factor of about 100. Such a value implies a mean neutrino energy of 400 MeV, which leads to the oscillation maximum at about 200 km for $\Delta m_{31}^2 = 2.4 \times 10^{-3} \text{ eV}^2$. We have checked that the performance at the somewhat shorter baseline of 130 km is rather similar to the one at the oscillation maximum. Moreover, the purpose of this paper is to estimate the physics potential for a realistic set-up and not to study the optimization of the β B regardless of any logistic consideration (see, e.g., refs. [40, 39] for such optimization studies).

The signal events from the $\nu_e \rightarrow \nu_\mu$ neutrino and antineutrino appearance channels in the β B are ν_μ charged current (CC) events. The Nuance v3r503 Monte Carlo code [33] is used to generate signal events. The selection for these events is based on standard Super-Kamiokande particle identification algorithms. The muon identification is reinforced by asking for the detection of the Michel decay electron. The neutrino energy is reconstructed by smearing momentum and direction of the charged lepton with the Super-Kamiokande resolution functions, and applying quasi-elastic (QE) kinematics assuming the known in-

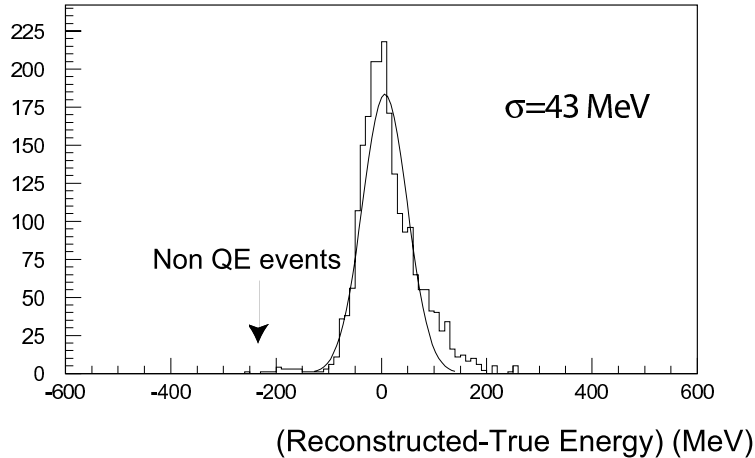


Figure 2: Energy resolution for ν_e interactions in the 200–300 MeV energy range. The quantity displayed is the difference between the reconstructed and the true neutrino energy.

coming neutrino direction. Energy reconstruction in the β B energy range is remarkably powerful (cf. also results of ref. [47]), and the contamination of non-QE events very small, as shown in figure 2. As pointed out in ref. [39], it is necessary to use a migration matrix for the neutrino energy reconstruction to properly handle Fermi motion smearing and the non-QE event contamination. We use 100 MeV bins for the reconstructed energy and 40 MeV bins for the true neutrino energy. Four migration matrices (for $\nu_e, \bar{\nu}_e, \nu_\mu, \bar{\nu}_\mu$) are applied to signal events as well as backgrounds. As suggested from figure 2 the results using migration matrices are very similar to a Gaussian energy resolution.

Backgrounds from charged pions and atmospheric neutrinos are computed with the identical analysis chain as signal events. Charged pions generated in NC events (or in NC-like events where the leading electron goes undetected) are the main source of background for the experiment. To compute this background inclusive NC and CC events have been generated with the β B spectrum. Events have been selected where the only visible track is a charged pion above the Čerenkov threshold. Particle identification efficiencies have been applied to those particles. The probability for a pion to survive in water until its decay has been computed with Geant 3.21 and cross-checked with a Fluka 2003 simulation. This probability is different for positive and negative pions, the latter having a higher probability to be absorbed before decaying. The surviving events are background, and the reconstructed neutrino energy is computed misidentifying these pions as muons. Event rates are reported in table 3. From these numbers it becomes evident that requiring the detection of the Michel electron provides an efficient cut to eliminate the pion background. These background rates are significantly smaller than quoted in ref. [37], where pion decays were computed with the same probabilities as for muons and they are slightly different from those quoted in ref. [49], where an older version of Nuance had been used. The numbers of table 3 have been cross-checked by comparing the Nuance and Neugen [50] event generators, finding a fair agreement in background rates and energy shape.

	^{18}Ne			^6He		
	ν_μ CC	π^+	π^-	$\bar{\nu}_\mu$ CC	π^+	π^-
Generated ev.	115367	557	341	101899	674	400
Particle ID	95717	204	100	85285	240	118
Decay	61347	107	8	69242	120	8

Table 3: Events for the βB in a 4400 kt yr exposure. ν_μ ($\bar{\nu}_\mu$) CC events are computed assuming full oscillations ($P_{\nu_e \rightarrow \nu_\mu} = 1$), and pion backgrounds are computed from ν_e ($\bar{\nu}_e$) CC+NC events. In the rows we give the number events generated within the fiducial volume (“Generated ev.”), after muon particle identification (“Particle ID”), and after applying a further identification requiring the detection of the Michel electron (“Decay”).

Also atmospheric neutrinos can constitute an important source of background [22, 39, 41, 49]. This background can be suppressed only by keeping a very short duty cycle ($2.2 \cdot 10^{-3}$ is the target value for the βB design study), and this in turn is one of the most challenging bounds on the design of the Beta Beam complex. Following ref. [49] we include the atmospheric neutrino background based on a Monte Carlo simulation using Nuance. Events are reconstructed as if they were signal neutrino events. We estimate that 5 events/year would survive the analysis chain in a full solar year (the βB should run for about 1/3 of this period) and include these events as backgrounds in the analysis. Under these circumstances, the present value of the βB duty cycle seems to be an overkill, it could be reduced by a factor 5 at least, see also ref. [49] for a discussion of the effect of a higher duty cycle.

3.3 The 3.5-GeV SPL Super Beam

In the recent Conceptual Design Report 2 (CDR2) the foreseen Super Proton Linac (SPL) [20] will provide the protons for the muon production in the context of a Neutrino Factory, and at a first stage will feed protons to a fixed target experiment to produce an intense conventional neutrino beam (“Super Beam”). The parameters of the beam line take into account the optimization [25] of the beam energy as well as the secondary particle focusing and decay to search for $\nu_\mu \rightarrow \nu_e$ and $\bar{\nu}_\mu \rightarrow \bar{\nu}_e$ appearance as well as ν_μ , $\bar{\nu}_\mu$ disappearance in a mega ton scale water Čerenkov detector. In particular, a full simulation of the beam line from the proton on target interaction up to the secondary particle decay tunnel has been performed. The proton on a liquid mercury target (30 cm long, 7.5 mm radius, 13.546 density) has been simulated with FLUKA 2002.4 [51] while the horn focusing system and the decay tunnel simulation has been preformed with GEANT 3.21 [52].¹

Since the optimization requirements for a Neutrino Factory are rather different than for a Super Beam the new SPL configuration has a significant impact on the physics

¹Although there are differences between the predicted pion and kaon productions as a function of proton kinetic energy with FLUKA 2002.4 and 2005.6, the results are consistent for the relevant energy of 3.5 GeV. We emphasize that the pion and the kaon production cross-sections are waiting for experimental confirmation [53] and a new optimization would be required if their is a disagreement with the present knowledge.

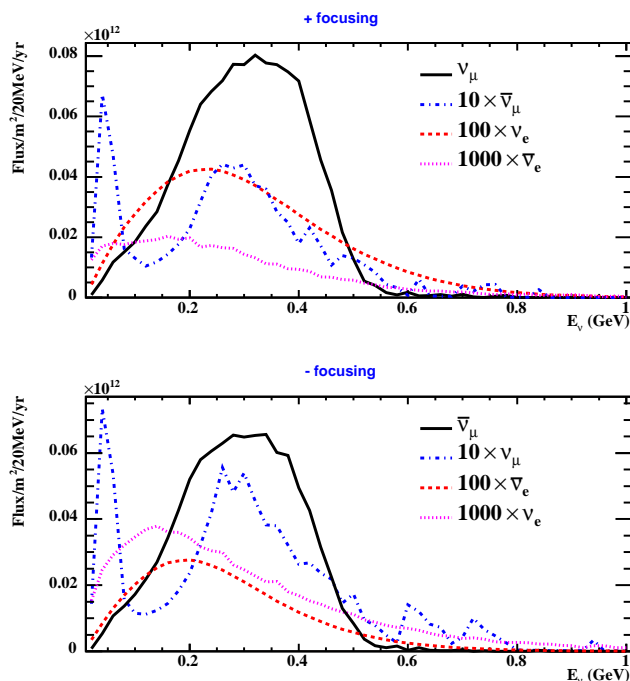


Figure 3: Neutrino fluxes, at 130 km from the target with the horns focusing the positive particles (top panel) or the negative particles (bottom panel). The fluxes are computed for a SPL proton beam of 3.5 GeV (4 MW), a decay tunnel with a length of 40 m and a radius of 2 m.

performance (see ref. [25] for a detailed discussion). The SPL fluxes of the four neutrino species (ν_μ , ν_e , $\bar{\nu}_\mu$, $\bar{\nu}_e$) for the positive (ν_μ beam) and the negative focusing ($\bar{\nu}_\mu$ beam) are shown in figure 3. The total number of ν_μ ($\bar{\nu}_\mu$) in positive (negative) focusing is about 1.18 (0.97) $\times 10^{12} \text{ m}^{-2} \text{ y}^{-1}$ with an average energy of 300 MeV. The ν_e ($\bar{\nu}_e$) contamination in the ν_μ ($\bar{\nu}_\mu$) beam is around 0.7% (6.0%). Following ref. [54], the π^0 background is reduced using a tighter PID cut compared to the standard Super-Kamiokande analysis used in K2K, but the cuts are looser than for T2K. Indeed, at SPL energies the π^0 background is less severe than for T2HK. This is because the resonant cross section is suppressed, and the produced pions have an energy where the angle between the two gammas is very wide, leading to a small probability that the two gamma rings overlap. This results in a higher signal efficiency of SPL compared to T2HK (70% against 40%) and a smaller rate of π^0 background. The Michel electron is required for the μ identification. For the $\nu_\mu \rightarrow \nu_e$ channel the background consists roughly of 90% $\nu_e \rightarrow \nu_e$ CC interactions, 6% π^0 from NC interactions, 3% miss identified muons from $\nu_\mu \rightarrow \nu_\mu$ CC, and 1% $\bar{\nu}_e \rightarrow \bar{\nu}_e$ CC interactions. For the $\bar{\nu}_\mu \rightarrow \bar{\nu}_e$ channel the contributions to the background are 45% $\bar{\nu}_e \rightarrow \bar{\nu}_e$ CC interactions, 35% $\nu_e \rightarrow \nu_e$ CC interactions, 18% π^0 from NC interactions and 2% miss identified muons from $\bar{\nu}_\mu \rightarrow \bar{\nu}_\mu$ CC. In addition we include the events from the contamination of “wrong sign” muon-neutrinos due to $\bar{\nu}_\mu \rightarrow \bar{\nu}_e$ ($\nu_\mu \rightarrow \nu_e$) oscillations in the neutrino (antineutrino) mode. We have checked that with the envisaged duty cycle of

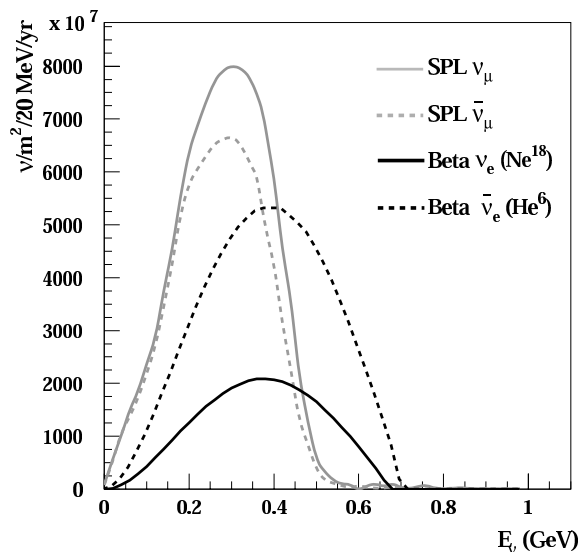


Figure 4: Comparison of the fluxes from SPL and β B.

2.4×10^{-4} the background from atmospheric neutrinos is negligible for the SPL.

Considering the signal over square-root of background ratio, the 3.5 GeV beam energy is more favorable than the original 2.2 GeV option. Compared to the fluxes used in refs. [54, 38] the gain is at least a factor 2.5 and this justifies to reconsider in detail the physics potential of the SPL Super Beam. Both the appearance and the disappearance channels are used. For the spectral analysis we use 10 bins of 100 MeV in the interval $0 < E_\nu < 1$ GeV, applying the same migration matrices as for the β B to take into account properly the neutrino energy reconstruction. As ultimate goal suggested in ref. [16] a 2% systematical error is used as default both for signal and background, this would be achieved by a special care of the design of the close position. However, we discuss also how a 5% systematical error affects the sensitivities. Using neutrino cross-sections on water from ref. [33], the number of expected ν_μ charged current is about 98 per kt yr. In figure 4 we compare the fluxes from the SPL to the one from the β B.

3.4 The atmospheric neutrino analysis

The simulation of atmospheric neutrino data in MEMPHYS is based on the analysis presented in ref. [30], with the following differences:

- We replace the neutrino fluxes at Kamioka with those at Gran Sasso. We use the Honda calculations [55], which unfortunately are not yet available for the Fréjus site. However, since the fluxes increase with the geomagnetic latitude and Fréjus is northern than Gran Sasso, our choice is conservative.
- We take into account the specific geometry of the MEMPHYS detector. This is particularly important to properly separate fully contained from partially contained events, as well as stopping muon from through-going muon events.

- We divide our total data sample into 420 different bins: fully contained single-ring events, further subdivided according to flavor (e -like or μ -like), lepton momentum (8 bins: 0.1–0.3, 0.3–0.5, 0.5–1, 1–2, 2–3, 3–5, 5–8, 8– ∞ GeV) and lepton direction (20 bins in zenith angle); fully contained multi-ring events, further subdivided according to flavor (e -like or μ -like), reconstructed neutrino energy (3 bins: 0–1.33, 1.33–5, 5– ∞ GeV) and lepton direction (10 bins in zenith angle); partially contained μ -like events, divided into 20 zenith bins; up-going muons, divided into stopping and through-going events, and in 10 zenith bins each.
- We include in our calculations the neutral-current contamination of each bin. To this extent we assume that the ratio between neutral-current and *unoscillated* charged-current events in MEMPHYS is the same as in Super-Kamiokande, and we take this ratio from ref. [3].
- We consider also multi-ring events, which we define as fully contained charged-current events which are *not* tagged as single-ring. Again, we assume that the survival efficiency and the NC contamination are the same as for Super-Kamiokande [3].

The expected number of contained events is given by:

$$N_b(\vec{\omega}) = N_b^{\text{NC}} + n_{\text{tgt}} T \sum_{\alpha, \beta, \pm} \int_0^\infty dh \int_{-1}^{+1} dc_\nu \int_{E_{\text{min}}}^\infty dE_\nu \int_{E_{\text{min}}}^{E_\nu} dE_l \int_{-1}^{+1} dc_a \int_0^{2\pi} d\varphi_a \quad (3.1)$$

$$\frac{d^3 \Phi_\alpha^\pm}{dE_\nu dc_\nu dh} (E_\nu, c_\nu, h) P_{\alpha \rightarrow \beta}^\pm (E_\nu, c_\nu, h | \vec{\omega}) \frac{d^2 \sigma_\beta^\pm}{dE_l dc_a} (E_\nu, E_l, c_a) \varepsilon_\beta^b (E_l, c_l(c_\nu, c_a, \varphi_a)),$$

where $P_{\alpha \rightarrow \beta}^+$ ($P_{\alpha \rightarrow \beta}^-$) is the $\nu_\alpha \rightarrow \nu_\beta$ ($\bar{\nu}_\alpha \rightarrow \bar{\nu}_\beta$) conversion probability for given values of the neutrino energy E_ν , the cosine c_ν of the angle between the incoming neutrino and the vertical direction, the production altitude h , and the neutrino oscillation parameters $\vec{\omega}$. We calculate the conversion probability numerically in the general three-flavor framework taking into account matter effects from a realistic Earth density profile. Further, N_b^{NC} is the neutral-current background for the bin b , n_{tgt} is the number of targets, T is the experiment running time, Φ_α^+ (Φ_α^-) is the flux of atmospheric neutrinos (antineutrinos) of type α , and σ_β^+ (σ_β^-) is the charged-current neutrino- (antineutrino-) nucleon interaction cross section. The variable E_l is the energy of the final lepton of type β , while c_a and φ_a parametrize the opening angle between the incoming neutrino and the final lepton directions as determined by the kinematics of the neutrino interaction. Finally, ε_β^b gives the probability that a charged lepton of type β , energy E_l and direction c_l contributes to the bin b .

Up-going muon events are calculated as follows:

$$N_b(\vec{\omega}) = \rho_{\text{rock}} T \sum_{\alpha, \pm} \int_0^\infty dh \int_{-1}^{+1} dc_\nu \int_{E_{\text{min}}}^\infty dE_\nu \int_{E_{\text{min}}}^{E_\nu} dE_\mu^0 \int_{E_{\text{min}}}^{E_\mu^0} dE_\mu^{\text{fin}} \int_{-1}^{+1} dc_a \int_0^{2\pi} d\varphi_a$$

$$\frac{d^3 \Phi_\alpha^\pm}{dE_\nu dc_\nu dh} (E_\nu, c_\nu, h) P_{\alpha \rightarrow \mu}^\pm (E_\nu, c_\nu, h | \vec{\omega}) \frac{d^2 \sigma_\mu^\pm}{dE_\mu^0 dc_a} (E_\nu, dE_\mu^0, c_a)$$

$$\times R_{\text{rock}}(E_\mu^0, E_\mu^{\text{fin}}) \mathcal{A}_{\text{eff}}^b (E_\mu^{\text{fin}}, c_l(c_\nu, c_a, \varphi_a)), \quad (3.2)$$

where ρ_{rock} is the density of targets in standard rock, R_{rock} is the effective muon range [56] for a muon which is produced with energy E_{μ}^0 and reaches the detector with energy E_{μ}^{fin} , and $\mathcal{A}_{\text{eff}}^b$ is the effective area for the bin b . The other variables and physical quantities are the same as for contained events.

The statistical analysis is based on the pull method, as described in ref. [57]. In our analysis we include three different kind of experimental uncertainties: Flux uncertainties: total normalization (20%), tilt factor (5%), zenith angle (5%), $\nu/\bar{\nu}$ ratio (5%), and μ/e ratio (5%); cross-section uncertainties: total normalization (15%) and μ/e ratio (1%) for each type of charged-current interaction (quasi-elastic, one-pion production, and deep-inelastic scattering), and total normalization (15%) for the neutral-current contributions; systematic uncertainties: same as in previous analyses, details are given in the appendix of ref. [57]. In addition, we assume independent normalization uncertainties (20%) for e -like and μ -like multi-ring events. Since we are dividing our data sample into a large number of bins, it is important to use Poisson statistics as some of the bins contain only a few number of events. We therefore write our χ^2 as:

$$\chi^2(\vec{\omega}) = \min_{\vec{\xi}} \left[2 \sum_b \left(N_b^{\text{th}}(\vec{\omega}, \vec{\xi}) - N_b^{\text{ex}} + N_b^{\text{ex}} \ln \frac{N_b^{\text{ex}}}{N_b^{\text{th}}(\vec{\omega}, \vec{\xi})} \right) + \sum_n \xi_n^2 \right], \quad (3.3)$$

where the number of events for a given value of the pulls $\vec{\xi}$ is given by:

$$N_b^{\text{th}}(\vec{\omega}, \vec{\xi}) = N_b^{\text{th}}(\vec{\omega}) \exp \left(\sum_n \pi_b^n(\vec{\omega}) \xi_n \right). \quad (3.4)$$

The use of an exponential dependence on the pulls in eq. (3.4), rather than the usual linear dependence, ensures that the theoretical predictions remain positive for *any* value of the pulls, thus avoiding numerical inconsistencies during the pull minimization procedure.

4. Degeneracies

A characteristic feature in the analysis of future LBL experiments is the presence of *parameter degeneracies*. Due to the inherent three-flavor structure of the oscillation probabilities, for a given experiment in general several disconnected regions in the multi-dimensional space of oscillation parameters will be present. Traditionally these degeneracies are referred to in the following way:

- The *intrinsic* or $(\delta_{\text{CP}}, \theta_{13})$ -degeneracy [58]: For a measurement based on the $\nu_{\mu} \rightarrow \nu_e$ oscillation probability for neutrinos and antineutrinos two disconnected solutions appear in the $(\delta_{\text{CP}}, \theta_{13})$ plane.
- The *hierarchy* or $\text{sign}(\Delta m_{31}^2)$ -degeneracy [59]: The two solutions corresponding to the two signs of Δm_{31}^2 appear in general at different values of δ_{CP} and θ_{13} .
- The *octant* or θ_{23} -degeneracy [60]: Since LBL experiments are sensitive mainly to $\sin^2 2\theta_{23}$ it is difficult to distinguish the two octants $\theta_{23} < \pi/4$ and $\theta_{23} > \pi/4$. Again, the solutions corresponding to θ_{23} and $\pi/2 - \theta_{23}$ appear in general at different values of δ_{CP} and θ_{13} .

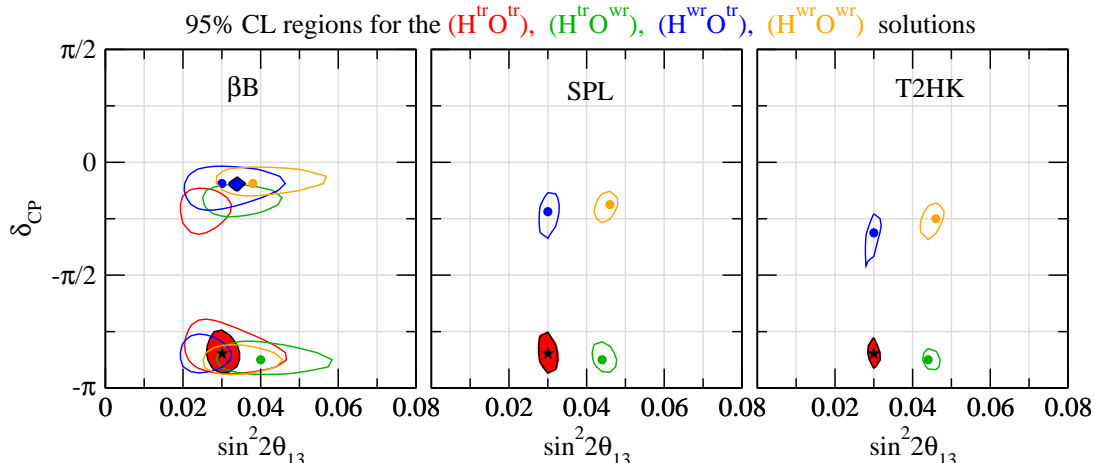


Figure 5: Allowed regions in $\sin^2 2\theta_{13}$ and δ_{CP} for LBL data alone (contour lines) and LBL+ATM data combined (colored regions). $\text{H}^{\text{tr/wr}}(\text{O}^{\text{tr/wr}})$ refers to solutions with the true/wrong mass hierarchy (octant of θ_{23}). The true parameter values are $\delta_{\text{CP}} = -0.85\pi$, $\sin^2 2\theta_{13} = 0.03$, $\sin^2 \theta_{23} = 0.6$, and the values from eq. (2.1) for the other parameters. The running time is $(5\nu + 5\bar{\nu})$ yrs for βB and $(2\nu + 8\bar{\nu})$ yrs for the Super Beams.

This leads to an eight-fold ambiguity in θ_{13} and δ_{CP} [61], and hence degeneracies provide a serious limitation for the determination of θ_{13} , δ_{CP} , and the sign of Δm_{31}^2 . Recent discussions of degeneracies can be found for example in refs. [32, 30, 62, 34]; degeneracies in the context of CERN-Fréjus βB and SPL have been considered previously in ref. [38]. In figure 5 we illustrate the effect of degeneracies for the βB , SPL, and T2HK experiments. Assuming the true parameter values $\delta_{\text{CP}} = -0.85\pi$, $\sin^2 2\theta_{13} = 0.03$, $\sin^2 \theta_{23} = 0.6$ we show the allowed regions in the plane of $\sin^2 2\theta_{13}$ and δ_{CP} taking into account the solutions with the wrong hierarchy and the wrong octant of θ_{23} .

As visible in figure 5 for the Super Beam experiments SPL and T2HK there is only a four-fold degeneracy related to $\text{sign}(\Delta m_{31}^2)$ and the octant of θ_{23} , whereas the intrinsic degeneracy can be resolved. Several pieces of information contribute to this effect, as we illustrate at the example of SPL in figure 6. The dashed curves in the left panel of this figure show the allowed regions for only the appearance measurement (for neutrinos and antineutrinos) without spectral information, i.e., just a counting experiment. In this case the eight-fold degeneracy is present in its full beauty, and one finds two solutions (corresponding to the intrinsic degeneracy) for each choice of $\text{sign}(\Delta m_{31}^2)$ and the octant of θ_{23} . Moreover, the allowed regions are relatively large. For the thin solid curves the information from the disappearance rate is added. The main effect is to decrease the size of the allowed regions in $\sin^2 2\theta_{13}$. This is especially pronounced for the solutions involving the wrong octant of θ_{23} , since these solutions are strongly affected by an uncertainty in θ_{23} which gets reduced by the disappearance information. Using in addition to the disappearance rate also the spectrum again decreases the size of the allowed regions, however, still all eight solutions are present (compare dashed curves in the right panel). The most relevant effect

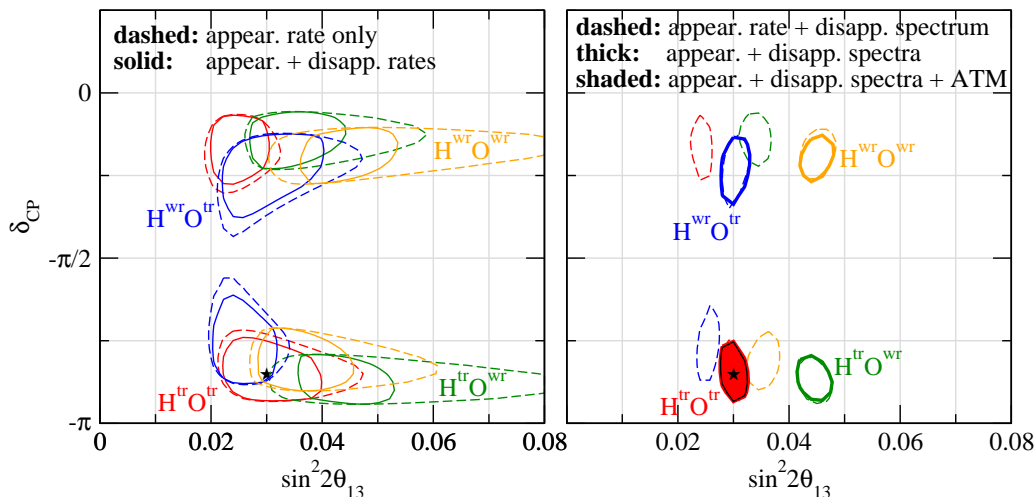


Figure 6: Resolving degeneracies in SPL by successively using the appearance rate measurement, disappearance channel rate and spectrum, spectral information in the appearance channel, and atmospheric neutrinos. Allowed regions in $\sin^2 2\theta_{13}$ and δ_{CP} are shown at 95% CL, and $H^{tr/wr}(O^{tr/wr})$ refers to solutions with the true/wrong mass hierarchy (octant of θ_{23}). The true parameter values are $\delta_{CP} = -0.85\pi$, $\sin^2 2\theta_{13} = 0.03$, $\sin^2 \theta_{23} = 0.6$, and the values from eq. (2.1) for the other parameters. The running time is $(2\nu + 8\bar{\nu})$ yrs.

comes from the inclusion of spectral information in the appearance channel, as visible from the comparison of the dashed and thick-solid curves in the right panel of figure 6. The intrinsic degeneracy gets resolved and only four solutions corresponding to the sign and octant degeneracies are left (see, e.g., refs. [32, 30, 34]).² Note that the thick curves in the right panel of figure 6 correspond to the regions show in figure 5 for the SPL. Finally, by the inclusion of information from atmospheric neutrinos all degeneracies can be resolved in this example, and the true solution is identified at 95% CL (see section 6.2 and ref. [30] for further discussions of atmospheric neutrinos).

Concerning the βB one observes from figure 5 that in this case the $(\delta_{CP}, \theta_{13})$ -degeneracy cannot be resolved and one has to deal with eight distinct solutions. One reason for this is the absence of precise information on $|\Delta m_{31}^2|$ and $\sin^2 2\theta_{23}$ which is provided by the ν_μ disappearance in Super Beam experiments but is not available from the βB . If external information on these parameters at the level of 3% is included the allowed regions in figure 5 are significantly reduced. However, still all eight solutions are present, which indicates that for the βB spectral information is not efficient enough to resolve the $(\delta_{CP}, \theta_{13})$ -degeneracy, and in this case only the inclusion of atmospheric neutrino data allows a nearly complete resolution of the degeneracies.

An important observation from figure 5 is that degeneracies have only a very small impact on the CP violation discovery, in the sense that if the true solution is CP violating also the fake solutions are located at CP violating values of δ_{CP} . Indeed, since for the

²The inclusion of spectral information might be the source of possible differences to previous studies, see e.g. ref. [38].

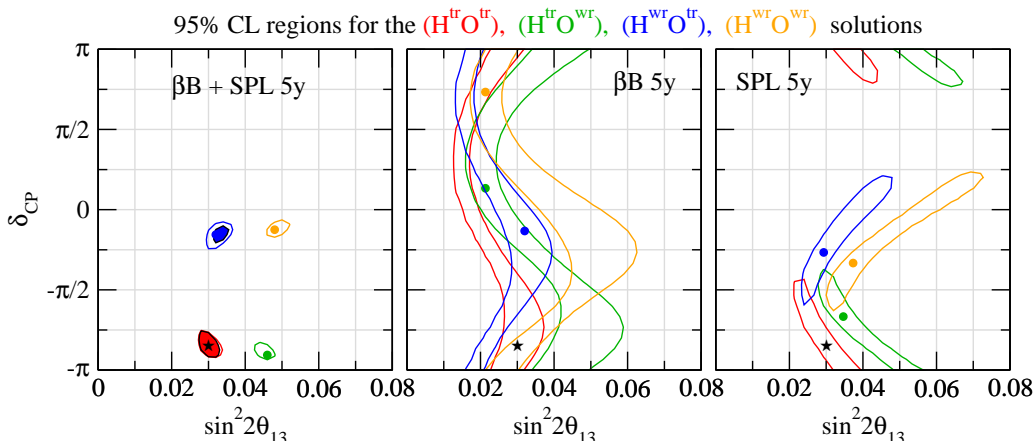


Figure 7: Allowed regions in $\sin^2 2\theta_{13}$ and δ_{CP} for 5 years data (neutrinos only) from βB , SPL, and the combination. $\text{H}^{\text{tr/wr}}(\text{O}^{\text{tr/wr}})$ refers to solutions with the true/wrong mass hierarchy (octant of θ_{23}). For the colored regions in the left panel also 5 years of atmospheric data are included; the solution with the wrong hierarchy has $\Delta\chi^2 = 4$. The true parameter values are $\delta_{\text{CP}} = -0.85\pi$, $\sin^2 2\theta_{13} = 0.03$, $\sin^2 \theta_{23} = 0.6$, and the values from eq. (2.1) for the other parameters. For the βB only analysis (middle panel) an external accuracy of 2% (3%) for $|\Delta m_{31}^2|$ (θ_{23}) has been assumed, whereas for the left and right panel the default value of 10% has been used.

relatively short baselines in the experiments under consideration matter effects are very small, the $\text{sign}(\Delta m_{31}^2)$ -degenerate solution is located within good approximation at $\delta'_{\text{CP}} \approx \pi - \delta_{\text{CP}}$ [59]. Therefore, although degeneracies strongly affect the determination of θ_{13} and δ_{CP} they have only a small impact on the CP violation discovery potential. Furthermore, as clear from figure 5 the $\text{sign}(\Delta m_{31}^2)$ degeneracy has practically no effect on the θ_{13} measurement, whereas the octant degeneracy has very little impact on the determination of δ_{CP} .

Figure 5 shows also that the fake solutions occur at similar locations in the $(\sin^2 2\theta_{13}, \delta_{\text{CP}})$ plane for βB and SPL. Therefore, as noted in ref. [38], in this sense the two experiments are not complementary, and the combination of 10 years of βB and SPL data is not very effective in resolving degeneracies. This is obvious since the baseline is the same and the neutrino energies are similar. Note however, that the βB looks for $\nu_e \rightarrow \nu_\mu$ appearance, whereas in SPL the T-conjugate channel $\nu_\mu \rightarrow \nu_e$ is observed. Assuming CPT invariance the relation $P_{\nu_\alpha \rightarrow \nu_\beta} = P_{\bar{\nu}_\beta \rightarrow \bar{\nu}_\alpha}$ holds, which implies that the antineutrino measurement can be replaced by a measurement in the T-conjugate channel. Hence, if βB and SPL experiments are available simultaneously the full information can be obtained just from neutrino data, and in principle the (time consuming) antineutrino measurement is not necessary. As shown in figure 7 the combination of 5 yrs neutrino data from the βB with 5 yrs of neutrino data from SPL leads to a result very close to the 10 yrs neutrino+antineutrino data from one experiment alone. Hence, if βB and SPL experiments are available simultaneously the data taking period is reduced approximately by a factor of 2 with respect to a single experiment. This synergy is discussed later in section 6.1 in the context of the θ_{13} and CP violation discovery potentials.

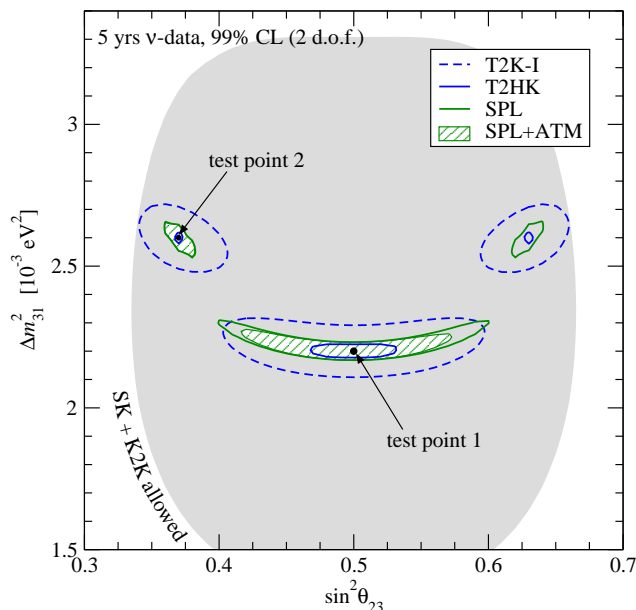


Figure 8: Allowed regions of Δm_{31}^2 and $\sin^2 \theta_{23}$ at 99% CL (2 d.o.f.) after 5 yrs of neutrino data taking for SPL, T2K phase I, T2HK, and the combination of SPL with 5 yrs of atmospheric neutrino data in the MEMPHYS detector. For the true parameter values we use $\Delta m_{31}^2 = 2.2$ (2.6) $\times 10^{-3} \text{ eV}^2$ and $\sin^2 \theta_{23} = 0.5$ (0.37) for the test point 1 (2), and $\theta_{13} = 0$ and the solar parameters as given in eq. (2.1). The shaded region corresponds to the 99% CL region from present SK and K2K data [12].

5. Physics potential

5.1 Sensitivity to the atmospheric parameters

The ν_μ disappearance channel available in the Super Beam experiments SPL and T2HK allows a precise determination of the atmospheric parameters $|\Delta m_{31}^2|$ and $\sin^2 2\theta_{23}$, see, e.g., refs. [63–65] for recent analyses). Figure 8 illustrates the improvement on these parameters by Super Beam experiments with respect to the present knowledge from SK atmospheric and K2K data. We show the allowed regions at 99% CL for T2K-I, SPL, and T2HK, where in all three cases 5 years of neutrino data are assumed. T2K-I corresponds to the phase I of the T2K experiment with a beam power of 0.77 MW and the Super-Kamiokande detector as target [16]. In table 4 we give the corresponding relative accuracies at 3σ for $|\Delta m_{31}^2|$ and $\sin^2 \theta_{23}$.

From the figure and the table it becomes evident that the T2K setups are very good in measuring the atmospheric parameters, and only a modest improvement is possible with SPL with respect to T2K phase I. T2HK provides an excellent sensitivity for these parameters, and for the example of the test point 2 sub-percent accuracies are obtained at 3σ . The disadvantage of SPL with respect to T2HK is the limited spectral information. Because of the lower beam energy nuclear Fermi motion is a severe limitation for energy reconstruction in SPL, whereas in T2K the somewhat higher energy allows an efficient use of spectral information of quasi-elastic events. Indeed, due to the large number of events in

	True values	T2K-I	SPL	T2HK
Δm_{31}^2	$2.2 \cdot 10^{-3} \text{ eV}^2$	4.7%	3.2%	1.1%
$\sin^2 \theta_{23}$	0.5	20%	20%	6%
Δm_{31}^2	$2.6 \cdot 10^{-3} \text{ eV}^2$	4.4%	2.5%	0.7%
$\sin^2 \theta_{23}$	0.37	8.9%	3.1%	0.8%

Table 4: Accuracies at 3σ on the atmospheric parameters $|\Delta m_{31}^2|$ and $\sin^2 \theta_{23}$ for 5 years of neutrino data from T2K-I, SPL, and T2HK for the two test points shown in figure 8 ($\theta_{13}^{\text{true}} = 0$). The accuracy for a parameter x is defined as $(x^{\text{upper}} - x^{\text{lower}})/(2x^{\text{true}})$, where x^{upper} (x^{lower}) is the upper (lower) bound at 3σ for 1 d.o.f. obtained by projecting the contour $\Delta\chi^2 = 9$ onto the x -axis. For the accuracies for test point 2 the octant degenerate solution is neglected.

the disappearance channel (cf. table 2) the measurement is completely dominated by the spectrum, and even increasing the normalization uncertainty up to 100% has very little impact on the allowed regions. The effect of spectral information on the disappearance measurement is discussed in some detail in ref. [65].

In the interpretation of the numbers given in table 4 one should consider that at accuracies below 1% systematics might become important, which are not accounted for here. We do include the most relevant systematics (see sections 2 and 3), however, at that level additional uncertainties related to, for example, the spectral shapes of signal and/or background, or the energy calibration might eventually limit the accuracy.

For the test point 1, with maximal mixing for θ_{23} , rather poor accuracies of $\sim 20\%$ for T2K-I and SPL, and 6% for T2HK are obtained for $\sin^2 \theta_{23}$. The reason is that in the disappearance channel $\sin^2 2\theta_{23}$ is measured with high precision, which translates to rather large errors for $\sin^2 \theta_{23}$ if $\theta_{23} = \pi/4$ [64]. For the same reason it is difficult to resolve the octant degeneracy, and for the test point 2, with a non-maximal value of $\sin^2 \theta_{23} = 0.37$, for all three LBL experiments the degenerate solution is present around $\sin^2 \theta_{23} = 0.63$. As pointed out in refs. [66, 67] atmospheric neutrino data may allow to distinguish between the two octants of θ_{23} . If 5 years of atmospheric neutrino data in MEMPHYS are added to the SPL data, the degenerate solution for the test point 2 can be excluded at more than 5σ and hence the octant degeneracy is resolved in this example, see section 6.2 for a more detailed discussion.

5.2 The θ_{13} discovery potential

If no finite value of θ_{13} is discovered by the next round of experiments an important task of the experiments under consideration here is to push further the sensitivity to this parameter. In this section we address this problem, where we use the following definition of the θ_{13} discovery potential: Data are simulated for a finite true value of $\sin^2 2\theta_{13}$ and a given true value for δ_{CP} . If the $\Delta\chi^2$ of the fit to these data with $\theta_{13} = 0$ is larger than 9 the corresponding true value of θ_{13} “is discovered at 3σ ”. In other words, the 3σ discovery limit as a function of the true δ_{CP} is given by the true value of $\sin^2 2\theta_{13}$ for which $\Delta\chi^2(\theta_{13} = 0) = 9$. In the fitting process we minimize the $\Delta\chi^2$ with respect to θ_{12} , θ_{23} ,

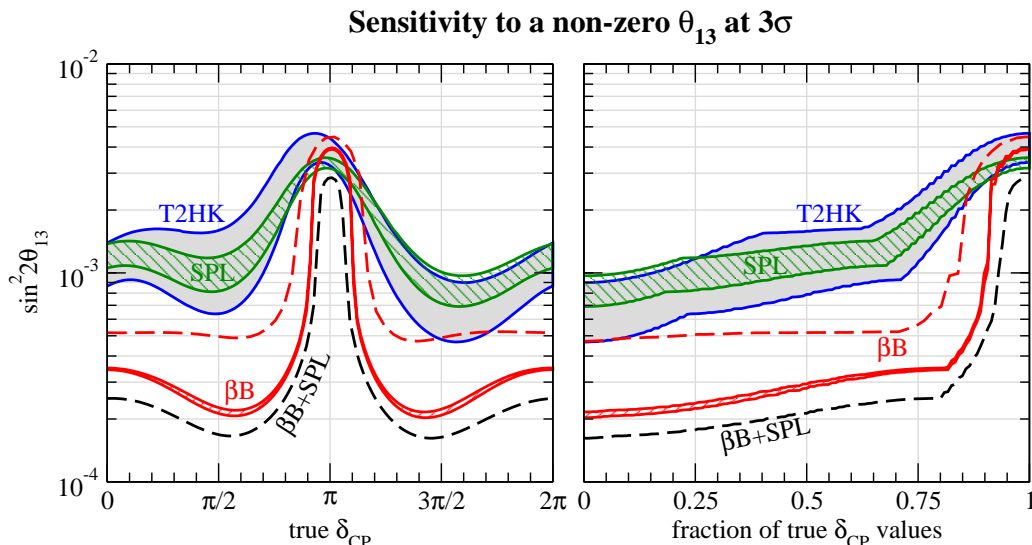


Figure 9: 3σ discovery sensitivity to $\sin^2 2\theta_{13}$ for β B, SPL, and T2HK as a function of the true value of δ_{CP} (left panel) and as a function of the fraction of all possible values of δ_{CP} (right panel). The running time is $(5\nu + 5\bar{\nu})$ yrs for β B and $(2\nu + 8\bar{\nu})$ yrs for the Super Beams. The width of the bands corresponds to values for the systematical errors between 2% and 5%. The black curves correspond to the combination of β B and SPL with 10 yrs of total data taking each for a systematical error of 2%, and the dashed curves show the sensitivity of the β B when the number of ion decays/yr are reduced by a factor of two with respect to the values given in table 1.

Δm_{12}^2 , and Δm_{31}^2 , and in general one has to test also for degenerate solutions in $\text{sign}(\Delta m_{31}^2)$ and the octant of θ_{23} .

The discovery limits are shown for β B, SPL, and T2HK in figure 9. One observes that SPL and T2HK are rather similar in performance, whereas the β B with our standard fluxes performs significantly better. For all three facilities a guaranteed discovery reach of $\sin^2 2\theta_{13} \simeq 5 \times 10^{-3}$ is obtained, irrespective of the actual value of δ_{CP} , however, for certain values of δ_{CP} the sensitivity is significantly improved. For SPL and T2HK discovery limits around $\sin^2 2\theta_{13} \simeq 10^{-3}$ are possible for a large fraction of all possible values of δ_{CP} , whereas for our standard β B a sensitivity below $\sin^2 2\theta_{13} = 4 \times 10^{-4}$ is reached for 80% of all possible values of δ_{CP} . If 10 years of data from β B and SPL are combined the discovery limit is dominated by the β B. Let us stress that the β B performance depends crucially on the neutrino flux intensity, as can be seen from the dashed curves in figure 9, which has been obtained by reducing the number of ion decays/yr by a factor of two with respect to our standard values given in table 1. In this case the sensitivity decreases significantly, but still values slightly better than from the Super Beam experiments are reached.

The peak of the sensitivity curves around $\delta_{\text{CP}} \approx \pi$ appears due to the interplay of neutrino and antineutrino data. For the Super Beams neutrino (antineutrino) data are most sensitive in the region $\pi \lesssim \delta_{\text{CP}} \lesssim 2\pi$ ($0 \lesssim \delta_{\text{CP}} \lesssim \pi$), and opposite for the β B, compare also figure 14 in section 6.1. The particular shape of the sensitivity curves emerges from the relative location of the corresponding curves for neutrino and antineutrino data, which

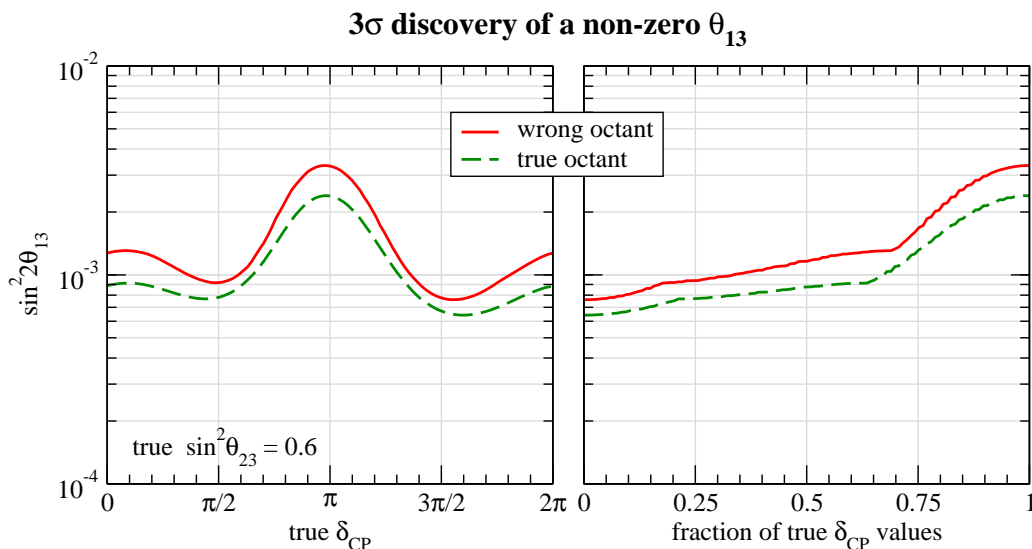


Figure 10: 3σ discovery sensitivity to $\sin^2 2\theta_{13}$ for the SPL as a function of the true value of δ_{CP} for $\sin^2 \theta_{23}^{\text{true}} = 0.6$ and true values for the other parameters as given in eq. (2.1). The running time is $(2\nu + 8\bar{\nu})$ yrs.

is controlled by the L/E_ν value where the experiment is operated and the value of $|\Delta m_{31}^2|$. The fact that the peak is most pronounced for the βB follows from the somewhat smaller L/E_ν of the βB compared to the Super Beams, whereas the shapes for SPL and T2HK are similar because of the similar L/E_ν values.

In figure 9 we illustrate also the effect of systematical errors on the θ_{13} discovery reach. The lower boundary of the band for each experiment corresponds to a systematical error of 2%, whereas the upper boundary is obtained for 5%. These errors include the (uncorrelated) normalization uncertainties on the signal as well as on the background, where the crucial uncertainty is the error on the background. We find that the βB is basically not affected by these errors, since the background has a rather different spectral shape (strongly peaked at low energies) than the signal. The fact that T2HK is relatively strongly affected by the actual value of the systematics can be understood by considering the ratio of signal to the square-root of the background using the numbers of table 2. We shall discuss this issue in more detail in the next section in the context of the CP violation discovery reach.

Let us remark that the θ_{13} sensitivities are practically not affected by the $\text{sign}(\Delta m_{31}^2)$ -degeneracy. This is easy to understand, since the data is fitted with $\theta_{13} = 0$, and in this case both mass hierarchies lead to very similar event rates. If the inverted hierarchy is used as the true hierarchy, the peak in the discovery limit visible in the left panel of figure 9 around $\delta_{CP} \sim \pi$ moves to $\delta_{CP} \sim 0$. However, the characteristic shape of the curves, and in particular, the sensitivity as a function of the δ_{CP} -fraction shown in the right panel are hardly affected by the sign of the true Δm_{31}^2 . In case of a non-maximal value of θ_{23} the octant-degeneracy has a minor impact on the θ_{13} discovery potential, as illustrated

in figure 10 for the SPL. We show the discovery limit obtained with the true and the fake octant of θ_{23} for a true value of $\sin^2 \theta_{23} = 0.6$. Let us note that for true values of $\sin^2 \theta_{23} > 0.5$ the octant-degenerate solution leads to a worse sensitivity to θ_{13} (see figure), whereas for $\sin^2 \theta_{23} < 0.5$ the fake solution does not affect the θ_{13} discovery, since in this case the sensitivity is increased.

5.3 Sensitivity to CP violation

In case a finite value of θ_{13} is established it is important to quantitatively assess the discovery potential for leptonic CP violation (CPV). The CP symmetry is violated if the complex phase δ_{CP} is different from 0 and π . Therefore, CPV is discovered if these values for δ_{CP} can be excluded. We evaluate the discovery potential for CPV in the following way: Data are calculated by scanning the true values of $\sin^2 2\theta_{13}$ and δ_{CP} . Then these data are fitted with the CP conserving values $\delta_{\text{CP}} = 0$ and $\delta_{\text{CP}} = \pi$, where all parameters except δ_{CP} are varied and the sign and octant degeneracies are taken into account. If no fit with $\Delta\chi^2 < 9$ is found CP conserving values of δ_{CP} can be excluded at 3σ for the chosen values of $\delta_{\text{CP}}^{\text{true}}$ and $\sin^2 2\theta_{13}^{\text{true}}$.

The CPV discovery potential for βB , SPL, and T2HK is shown in figure 11. As in the case of the θ_{13} sensitivity we find that SPL and T2HK perform rather similar, whereas the βB has significantly better sensitivity if our adopted numbers of ion decays per year can be achieved. For systematical errors of 2% maximal CPV (for $\delta_{\text{CP}}^{\text{true}} = \pi/2, 3\pi/2$) can be discovered at 3σ down to $\sin^2 2\theta_{13} \simeq 8.8(6.6) \times 10^{-4}$ for SPL (T2HK), and $\sin^2 2\theta_{13} \simeq 2 \times 10^{-4}$ for the βB . This number for the βB is increased by a factor 3 if the fluxes are reduced to half of our nominal values. The best sensitivity to CPV is obtained for all three facilities around $\sin^2 2\theta_{13} \sim 10^{-2}$. For this value CPV can be established for 78%, 73%, 75% of all values of δ_{CP} for βB , SPL, T2HK, respectively (again for systematics of 2%).

The widths of the bands in figure 11 corresponds to different values for systematical errors. The curves which give the best sensitivities are obtained for systematics of 2%, the curves corresponding to the worst sensitivity have been computed for systematics of 5%. We change the uncertainty on the signal as well as on the background, however, it turns out that the most relevant uncertainty is the background normalization. We find that the impact of systematics is very small for the βB . The reason for this is that the spectral shape of the background in the βB (from pions and atmospheric neutrinos) is very different from the signal, and therefore they can be disentangled by the fit of the energy spectrum. For the Super Beams the background spectrum is more similar to the signal, and therefore an uncertainty on the background normalization might have a strong impact on the sensitivity, as visible from the SPL and T2HK curves in figure 11. In particular T2HK is strongly affected, and moving from 2% to 5% uncertainty decreases the sensitivity to maximal CPV by a factor 3.

This interesting feature can be understood in the following way. A rough measure to estimate the sensitivity is given by the signal compared to the error on the background. The latter receives contributions from the statistical error \sqrt{B} and from the systematical uncertainty $\sigma_{\text{bkg}} B$, where B is the number of background events and σ_{bkg} is the (relative) systematical error. Hence the importance of the systematics can be estimated by the ratio

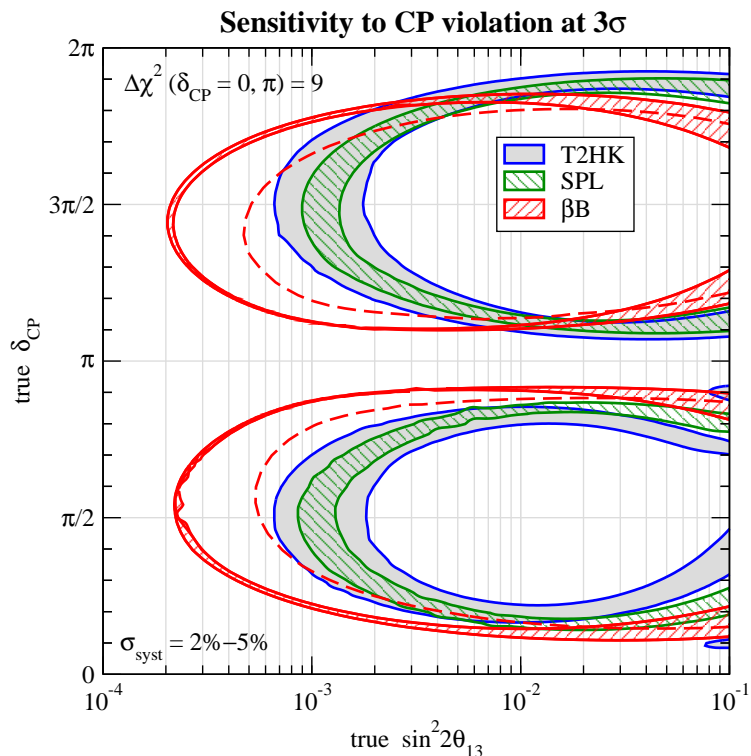


Figure 11: CPV discovery potential for β B, SPL, and T2HK: For parameter values inside the ellipse-shaped curves CP conserving values of δ_{CP} can be excluded at 3σ ($\Delta\chi^2 > 9$). The running time is $(5\nu + 5\bar{\nu})$ yrs for β B and $(2\nu + 8\bar{\nu})$ yrs for the Super Beams. The width of the bands corresponds to values for the systematical errors from 2% to 5%. The dashed curves show the sensitivity of the β B when the number of ion decays/yr are reduced by a factor of two with respect to the values given in table 1 for 2% systematics.

of systematical and statistical errors $\sigma_{\text{bkgr}}B/\sqrt{B} = \sigma_{\text{bkgr}}\sqrt{B}$. Summing the numbers for background events in the neutrino and antineutrino channels given in table 2 one finds that systematical errors dominate ($\sigma_{\text{bkgr}}\sqrt{B} > 1$) if $\sigma_{\text{bkgr}} \gtrsim 6\%$, 3% , 2% for β B, SPL, T2HK, respectively. In the right panel figure 12 we show the sensitivity to maximal CPV (as defined in the figure caption) as a function of σ_{bkgr} . Indeed, the worsening of the sensitivity due to systematics occurs roughly at the values of σ_{bkgr} as estimated above. For a more quantitative understanding of these curves it is necessary to consider the number of signal and background events for neutrinos and antineutrinos separately, as well as to take into account spectral information.

The left panel of figure 12 shows the sensitivity to maximal CPV as a function of the exposure³ for values of σ_{bkgr} from 2% to 5%. One can observe clearly that for the standard

³Note that the CPV sensitivity for the β B with reduced fluxes from figure 11 is worse than the value which follows from figure 12. The reason is that in figure 12 the total exposure is scaled (mass \times time), i.e., signal and background are scaled in the same way, whereas for the dashed curve in figure 11 only the fluxes are reduced but backgrounds are kept constant.

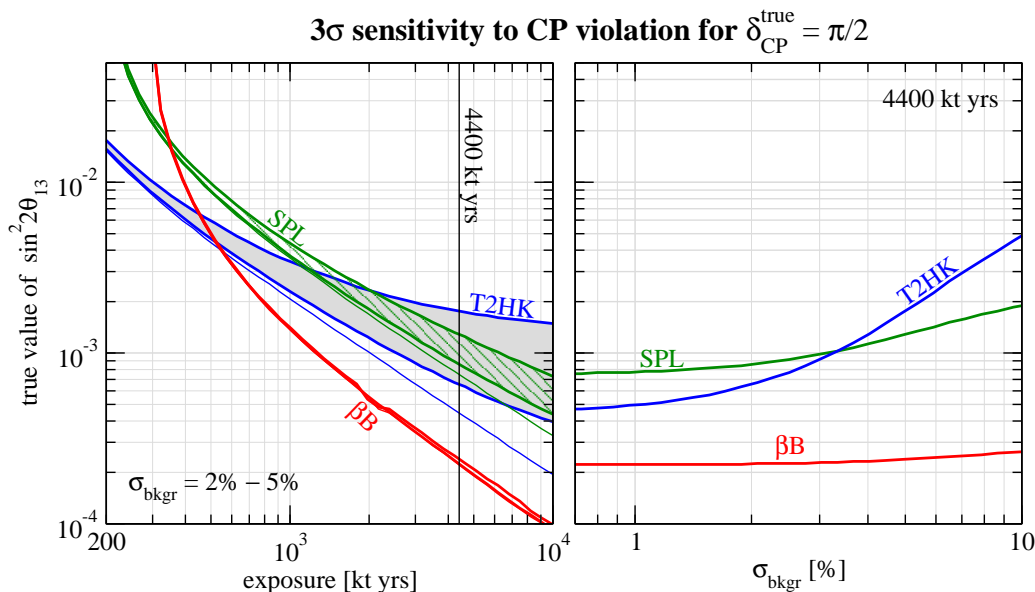


Figure 12: Impact of total exposure and systematical errors on the CPV discovery potential of βB , SPL, and T2HK. We show the smallest true value of $\sin^2 2\theta_{13}$ for which $\delta_{\text{CP}} = \pi/2$ can be distinguished from $\delta_{\text{CP}} = 0$ or $\delta_{\text{CP}} = \pi$ at 3σ ($\Delta\chi^2 > 9$) as a function of the exposure in kt yrs (left) and as a function of the systematical error on the background σ_{bkgr} (right). The widths of the curves in the left panel corresponds to values of σ_{bkgr} from 2% to 5%. The thin solid curves in the left panel corresponds to no systematical errors. The right plot is calculated for the standard exposure of 4400 kt yrs. No systematical error on the signal has been assumed.

exposure of 4400 kt yrs T2HK is dominated by systematics and changing σ_{bkgr} from 2% to 5% has a big impact on the sensitivity. In contrast the CERN-MEMPHYS experiments (especially the βB) are rather stable with respect to systematics and for the standard exposure they are still statistics dominated. We conclude that in T2HK systematics have to be under very good control, whereas this issue is less important for βB and SPL. We have checked explicitly that the systematical error on the signal has negligible impact on these results. Therefore, we have set this error to zero for calculating figure 12 to highlight the importance of the background error. In all other calculations also the signal error is included, in particular also in figure 11.

Let us remark that for the T2KK configuration (with one half of the Hyper-K detector mass at Kamioka and the second half at the same off-axis angle in Korea) the problem of systematics might be less severe than for T2HK, since both detectors observe the same flux and background. Note however, that an important issue for the CPV sensitivity is whether systematics between neutrino and antineutrino data are correlated or not. We have checked that the worse sensitivities for T2HK shown in figure 11 compared to the results obtained in refs. [34, 35] can be traced back to the fact that in these papers neutrino and antineutrino systematics are correlated, whereas we consider them to be independent. Note that our approach is conservative, and the assumption of uncorrelated errors has been adopted also

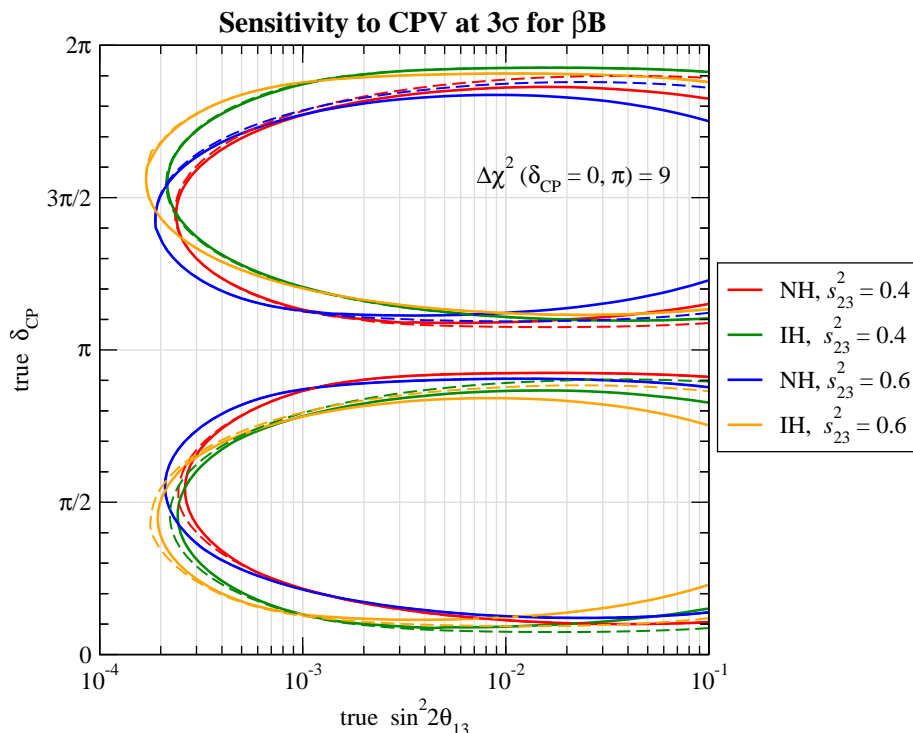


Figure 13: Impact of degeneracies on the CPV discovery potential for the βB . We show the sensitivity to CPV at 3σ ($\Delta\chi^2 > 9$) computed for 4 different combinations of the true values of the hierarchy (NH or IH) and θ_{23} ($\sin^2\theta_{23} = 0.4$ or 0.6). Dashed curves are computed neglecting degeneracies in the fit. The running time is $(5\nu + 5\bar{\nu})$ yrs.

for the CERN-MEMPHYS experiments.

Finally, in figure 13 we illustrate the impact of degeneracies, as well as the true hierarchy and θ_{23} -octant on the CPV sensitivity. Curves of different colors correspond to the four different choices for $\text{sign}(\Delta m_{31}^2)$ and the θ_{23} -octant of the true parameters. For the solid curves the simulated data for each choice of true $\text{sign}(\Delta m_{31}^2)$ and θ_{23} -octant are fitted by taking into account all four degenerate solutions, i.e., also for the fit all four combinations of $\text{sign}(\Delta m_{31}^2)$ and θ_{23} -octant are used. One observes from the figure that the true hierarchy and octant have a rather small impact on the βB CPV sensitivity, in particular the sensitivity to maximal CPV is completely independent. The main effect of changing the true hierarchy is to exchange the behavior between $0 < \delta_{CP} < 180^\circ$ and $180^\circ < \delta_{CP} < 360^\circ$. For $\sin^2 2\theta_{13} \lesssim 10^{-2}$ the sensitivity gets slightly worse if $\theta_{23}^{\text{true}} > \pi/4$ compared to $\theta_{23}^{\text{true}} < \pi/4$.

The dashed curves in figure 13 are computed without taking into account the degeneracies, i.e., for each choice of true $\text{sign}(\Delta m_{31}^2)$ and θ_{23} -octant the data are fitted only with this particular choice. The effect of the degeneracies becomes visible for large values of θ_{13} . Note that this is just the region where they can be reduced by a combined analysis with atmospheric neutrinos (see section 6.2 or ref. [30]).

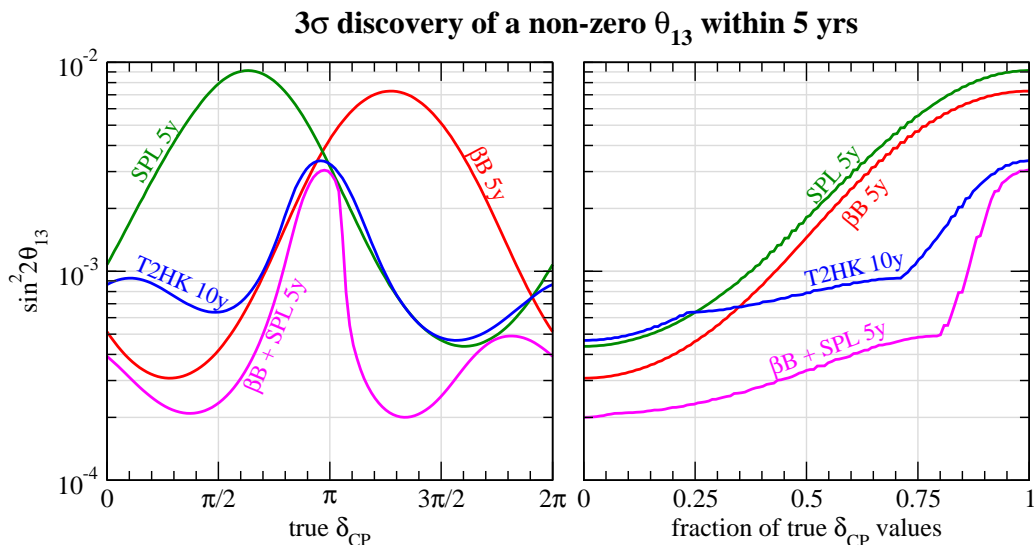


Figure 14: Discovery potential of a finite value of $\sin^2 2\theta_{13}$ at 3σ ($\Delta\chi^2 > 9$) for 5 yrs neutrino data from β B, SPL, and the combination of β B + SPL compared to 10 yrs data from T2HK (2 yrs neutrinos + 8 yrs antineutrinos).

6. Synergies provided by the CERN-MEMPHYS facilities

6.1 Combining Beta Beam and Super Beam

In this section we discuss synergies which emerge if both β B and SPL are available. The main difference between these two beams is the different initial neutrino flavor, $\bar{\nu}_e$ for β B and $\bar{\nu}_\mu$ for SPL. This implies that at near detectors all relevant cross sections can be measured. In particular, the near detector of the β B will measure the cross section for the SPL appearance search, and vice versa. If both experiments run with neutrinos and antineutrinos all possible transition probabilities are covered: $P_{\nu_e \rightarrow \nu_\mu}$, $P_{\bar{\nu}_e \rightarrow \bar{\nu}_\mu}$, $P_{\nu_\mu \rightarrow \nu_e}$, and $P_{\bar{\nu}_\mu \rightarrow \bar{\nu}_e}$. Together with the fact that matter effects are very small because of the relatively short baseline, this means that in addition to CP also direct tests of the T and CPT symmetries are possible.

However, if the CPT symmetry is assumed in principle all information can be obtained just from neutrino data because of the relations $P_{\bar{\nu}_e \rightarrow \bar{\nu}_\mu} = P_{\nu_\mu \rightarrow \nu_e}$ and $P_{\bar{\nu}_\mu \rightarrow \bar{\nu}_e} = P_{\nu_e \rightarrow \nu_\mu}$. As mentioned already in section 4 this implies that (time consuming) antineutrino running can be avoided. We illustrate this synergy in figures 14 and 15. In figure 14 we show the θ_{13} discovery potential of 5 years of neutrino data from β B and SPL. From the left panel the complementarity of the two experiments is obvious, since each of them is most sensitive in a different region of δ_{CP} . (As expected from general properties of the oscillation probabilities the sensitivity curves of β B and SPL are approximately related by the transformation $\delta_{CP} \rightarrow 2\pi - \delta_{CP}$.) Combining these two data sets results in a sensitivity slightly better than from 10 years ($2\nu + 8\bar{\nu}$) of T2HK data. As visible in figure 15 also for the CPV discovery this synergy works and 5 years of neutrino data from β B and SPL lead to a

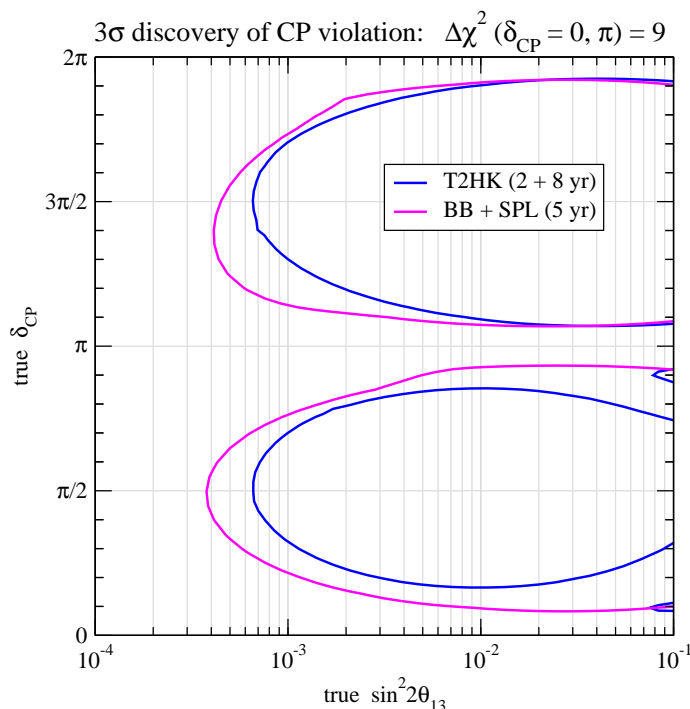


Figure 15: Sensitivity to CPV at 3σ ($\Delta\chi^2 > 9$) for combining 5 yrs neutrino data from βB and SPL compared to 10 yrs data from T2HK (2 yrs neutrinos + 8 yrs antineutrinos).

similar sensitivity as 10 years of T2HK.

6.2 Resolving degeneracies with atmospheric neutrinos

It was pointed out in ref. [30] that for LBL experiments based on mega ton scale water Čerenkov detectors data from atmospheric neutrinos (ATM) provide an attractive method to resolve degeneracies. Atmospheric neutrinos are sensitive to the neutrino mass hierarchy if θ_{13} is sufficiently large due to Earth matter effects, mainly in multi-GeV e -like events [68–70]. Moreover, sub-GeV e -like events provide sensitivity to the octant of θ_{23} [71, 66, 67] due to oscillations with Δm_{21}^2 (see also ref. [72] for a discussion of atmospheric neutrinos in the context of Hyper-K). Following ref. [30] we investigate here the synergy from a combination of LBL data from βB and SPL with ATM data in the MEMPHYS detector. Technical details are given in section 3.4.

The effect of degeneracies in LBL data has been discussed in section 4, see figures 5 and 6. As discussed there, for given true parameter values the data can be fitted with the wrong hierarchy and/or with the wrong octant of θ_{23} . Hence, from LBL data alone the hierarchy and the octant cannot be determined and ambiguities exist in the determination of θ_{13} and δ_{CP} . If the LBL data are combined with ATM data only the colored regions in figure 5 survive, i.e., in this particular example for SPL and T2HK the degeneracies are completely lifted at 95% CL, the mass hierarchy and the octant of θ_{23} can be identified, and the ambiguities in θ_{13} and δ_{CP} are resolved. For the βB an island corresponding to

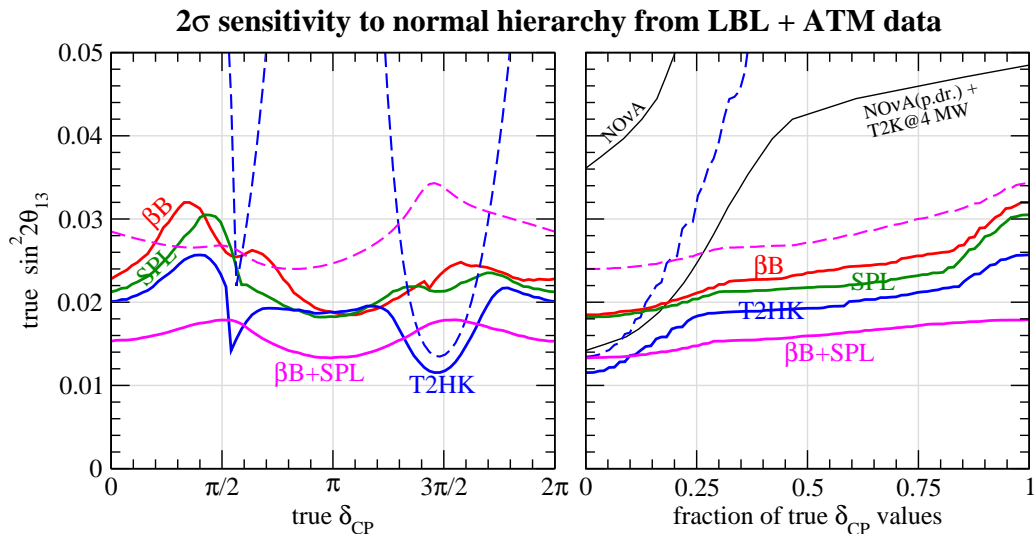


Figure 16: Sensitivity to the mass hierarchy at 2σ ($\Delta\chi^2 = 4$) as a function of the true values of $\sin^2 2\theta_{13}$ and δ_{CP} (left), and the fraction of true values of δ_{CP} (right). The solid curves are the sensitivities from the combination of long-baseline and atmospheric neutrino data, the dashed curves correspond to long-baseline data only. The running time is $(5\nu + 5\bar{\nu})$ yrs for βB and $(2\nu + 8\bar{\nu})$ yrs for the Super Beams. For comparison we show in the right panel also the sensitivities of $\text{NO}\nu\text{A}$ and $\text{NO}\nu\text{A}+\text{T2K}$ extracted from figure 13.14 of ref. [17]. For the curve labeled “ $\text{NO}\nu\text{A}$ (p.dr.)+ $\text{T2K}@4$ MW” a proton driver has been assumed for $\text{NO}\nu\text{A}$ and the T2K beam has been up-graded to 4 MW, see ref. [17] for details.

the wrong hierarchy does survive at the 95% CL for 2 dof. Still, the solution with the wrong sign of Δm_{31}^2 is disfavored with $\Delta\chi^2 = 5.1$ with respect to the true solution, which corresponds to 2.4σ for 1 dof. Let us note that in figure 5 we have chosen a favorable value of $\sin^2 \theta_{23} = 0.6$; for values $\sin^2 \theta_{23} < 0.5$ in general the sensitivity of ATM data is weaker [30].

In figure 16 we show how the combination of ATM+LBL data leads to a non-trivial sensitivity to the neutrino mass hierarchy, i.e. to the sign of Δm_{31}^2 . For LBL data alone (dashed curves) there is practically no sensitivity for the CERN-MEMPHYS experiments (because of the very small matter effects due to the relatively short baseline), and the sensitivity of T2HK depends strongly on the true value of δ_{CP} . However, by including data from atmospheric neutrinos (solid curves) the mass hierarchy can be identified at 2σ CL provided $\sin^2 2\theta_{13} \gtrsim 0.02 - 0.03$. As an example we have chosen in that figure a true value of $\theta_{23} = \pi/4$. Generically the hierarchy sensitivity increases with increasing θ_{23} , see ref. [30] for a detailed discussion.

The sensitivity to the neutrino mass hierarchy shown in figure 16 is significantly improved with respect to our previous results obtained in ref. [30]. There are two main reasons for this improved performance: First, we use now much more bins in charged lepton energy for fully contained single-ring events⁴ (compare section 3.4), and second, we implemented

⁴The impact of energy binning on the hierarchy determination with atmospheric neutrinos has been

also information from multi-ring events. This latter point is important since the relative contribution of neutrinos and antineutrinos is different for single- and multi-ring events. Therefore, combining single- and multi-ring data allows to obtain a discrimination between neutrino and antineutrino events on a statistical basis. This in turn contains crucial information on the hierarchy, since the matter enhancement is visible either in neutrinos or antineutrinos, depending on the hierarchy.

Although βB and SPL alone have no sensitivity to the hierarchy at all, we find that the combination of them does provide rather good sensitivity even without atmospheric data. The reason for this interesting effect is the following. Because of the rather short baseline the matter effect is too small to distinguish between NH and IH given only neutrino and antineutrino information in one channel. However, the tiny matter effect suffices to move the hierarchy degenerate solution to slightly different locations in the $(\sin^2 2\theta_{13}, \delta_{\text{CP}})$ plane for the $\bar{\nu}_e \rightarrow \bar{\nu}_\mu$ (βB) and $\bar{\nu}_\mu \rightarrow \bar{\nu}_e$ (SPL) channels (compare figure 5). Hence, if all four CP and T conjugate channels are available (as it is the case for the $\beta\text{B}+\text{SPL}$ combination) already the small matter effect picked up along the 130 km CERN-MEMPHYS distance provides sensitivity to the mass hierarchy for $\sin^2 2\theta_{13} \gtrsim 0.03$, or $\sin^2 2\theta_{13} \gtrsim 0.015$ if also atmospheric neutrino data is included.

For comparison we show in the right panel of figure 16 also the sensitivity of the NO ν A [17] experiment, and of NO ν A+T2K, where in the second case a beam upgrade by a proton driver has been assumed for NO ν A, and for T2K the Super-Kamiokande detector has been used but the beam intensity has been increased by assuming 4 MW power. More details on these sensitivities can be found in ref. [17]. Let us note that in general LBL experiments with two detectors and/or very long baselines ($\gtrsim 1000$ km) are a competitive method to atmospheric neutrinos for the hierarchy determination, see, e.g., refs. [34, 35, 74, 36, 75] for recent analyses. In particular, in case of the T2KK extension of the T2HK experiment, the very long baseline to Korea allows for a determination of the mass hierarchy down to $\sin^2 2\theta_{13} \gtrsim 0.02$ (2σ) without using atmospheric neutrinos [35]. We mention also the possibility to determine the neutrino mass hierarchy by using neutrino events from a galactic Super Nova explosion in mega ton Čerenkov detectors such as MEMPHYS, see, e.g., ref. [76].

Figure 17 shows the potential of ATM+LBL data to exclude the octant degenerate solution. Since this effect is based mainly on oscillations with Δm_{21}^2 there is very good sensitivity even for $\theta_{13} = 0$; a finite value of θ_{13} in general improves the sensitivity [30]. From the figure one can read off that atmospheric data alone can resolve the correct octant at 3σ if $|\sin^2 \theta_{23} - 0.5| \gtrsim 0.085$. If atmospheric data is combined with the LBL data from SPL or T2HK there is sensitivity to the octant for $|\sin^2 \theta_{23} - 0.5| \gtrsim 0.05$. The improvement of the octant sensitivity with respect to previous analyses [30, 67] follows from changes in the analysis of sub-GeV atmospheric events, where now three bins in lepton momentum are used instead of one. Note that since in figure 17 we have assumed a true value of $\theta_{13} = 0$, combining the βB with ATM does not improve the sensitivity with respect to atmospheric data alone. We note that the T2KK configuration provides also

discussed recently in ref. [73] in the context of magnetized iron detectors.

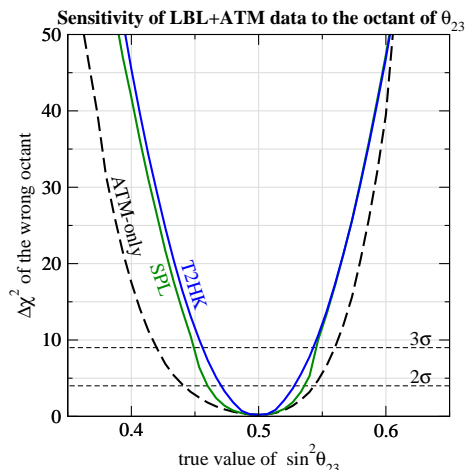


Figure 17: $\Delta\chi^2$ of the solution with the wrong octant of θ_{23} as a function of the true value of $\sin^2 \theta_{23}$. We have assumed a true value of $\theta_{13} = 0$, and the running time is $(2\nu + 8\bar{\nu})$ yrs.

some sensitivity to the octant of θ_{23} without referring to atmospheric neutrinos. In ref. [35] it was found that for $|\sin^2 \theta_{23} - 0.5| \gtrsim 0.12$ the octant can be identified in T2KK at 3σ .

7. Summary

In this work we have studied the physics potential of the CERN-MEMPHYS neutrino oscillation project. We consider a Beta Beam (βB) with $\gamma = 100$ for the stored ions, where existing facilities at CERN can be used optimally, and a Super Beam based on an optimized Super Proton Linac (SPL) with a beam energy of 3.5 GeV and 4 MW power. As target we assume the MEMPHYS detector, a 440 kt water Čerenkov detector at Fréjus, at a distance of 130 km from CERN. The main characteristics of the experiments are summarized in table 1. The adopted neutrino fluxes are based on realistic calculations of ion production and storage for the βB , and a full simulation of the beam line (particle production and decay of secondaries) for SPL. Special care has been given to the issue of backgrounds, which we include by means of detailed event simulations and applying Super-Kamiokande particle identification algorithms.

The physics potential of the βB and SPL experiments in terms of θ_{13} discovery reach and sensitivity to CP violation has been addressed where parameter degeneracies are fully taken into account. The main results on these performance indicators are summarized in figures 9 and 11. We obtain a guaranteed discovery reach of $\sin^2 2\theta_{13} \simeq 5 \times 10^{-3}$ at 3σ , irrespective of the actual value of δ_{CP} . For certain values of δ_{CP} the sensitivity is significantly improved, and for βB (SPL) discovery limits around $\sin^2 2\theta_{13} \simeq 3(10) \times 10^{-4}$ are possible for a large fraction of all possible values of δ_{CP} . Maximal CP violation (for $\delta_{CP}^{\text{true}} = \pi/2, 3\pi/2$) can be discovered at 3σ down to $\sin^2 2\theta_{13} \simeq 2(9) \times 10^{-4}$ for βB (SPL), whereas the best sensitivity to CP violation is obtained for $\sin^2 2\theta_{13} \sim 10^{-2}$: For $\sin^2 2\theta_{13} = 10^{-2}$ CP violation can be established at 3σ for 78% (73%) of all possible true values of

δ_{CP} for βB (SPL). We stress that the βB performance in general depends crucially on the number of ion decays per year. The impact of the value of systematical uncertainties on signal and background on our results is discussed. The βB and SPL sensitivities are compared to the ones of the phase II of the T2K experiment in Japan (T2HK), which is a competing proposal of similar size and timescale. In general we obtain rather similar sensitivities for T2HK and SPL, and hence the CERN-MEMPHYS experiments provide a viable alternative to T2HK. We find that βB and SPL are less sensitive to systematical errors, whereas the sensitivity of T2HK crucially depends on the systematical error on the background.⁵

Assuming that both βB and SPL experiments are available, we point out that one can benefit from the different oscillation channels $\nu_e \rightarrow \nu_\mu$ for βB and $\nu_\mu \rightarrow \nu_e$ for SPL, since by the combination of these channels the time intensive antineutrino measurements can be avoided. We show that 5 years of neutrino data from βB and SPL lead to similar results as 2 years of neutrino plus 8 years of antineutrino data from T2HK. Furthermore, we discuss the use of atmospheric neutrinos in the MEMPHYS detector to resolve parameter degeneracies in the long-baseline data. This effect leads to a sensitivity to the neutrino mass hierarchy at 2σ CL for $\sin^2 2\theta_{13} \gtrsim 0.025$ for βB and SPL, although these experiments alone (without atmospheric data) have no sensitivity at all. The optimal hierarchy sensitivity is obtained from combining $\beta\text{B}+\text{SPL}+\text{atmospheric}$ data. Furthermore, the combination of atmospheric data with a Super Beam provides a possibility to determine the octant of θ_{23} .

To conclude, we have shown that the CERN-MEMPHYS neutrino oscillation project based on a Beta Beam and/or a Super Beam plus a mega ton scale water Čerenkov detector offers interesting and competitive physics possibilities and is worth to be considered as a serious option in the worldwide process of identifying future high precision neutrino oscillation facilities [77].

Acknowledgments

We thank J. Argyriades for communication on the Super-K atmospheric neutrino analysis, A. Cazes for his work on the SPL simulation, and P. Huber for his patience in answering questions concerning the use of GLoBES. Furthermore, we thank D. Casper for the help in installing and running Nuance, and E. Couce for discussions about the βB backgrounds. T.S. is supported by the 6th Framework Program of the European Community under a Marie Curie Intra-European Fellowship.

References

- [1] B.T. Cleveland et al., *Measurement of the solar electron neutrino flux with the homestake chlorine detector*, *Astrophys. J.* **496** (1998) 505;
SAGE collaboration, J.N. Abdurashitov et al., *Measurement of the solar neutrino capture rate by the russian-american Gallium solar neutrino experiment during one half of the*

⁵Let us note that in the present study we have not considered the recent “T2KK” proposal [34], where one half of the Hyper-K detector mass is at Kamioka and the second half in Korea. For such a setup our results do not apply and especially the conclusion on systematical errors may be different.

- 22-year cycle of solar activity, *Sov. Phys. JETP* **95** (2002) 181 [*Zh. Eksp. Teor. Fiz.* **122** (2002) 211] [astro-ph/0204245];
 GALLEX and GNO collaboration, T. Kirsten et al., *Progress in GNO Nucl. Phys.* **118** (Proc. Suppl.) (2003) 33;
 SUPER-KAMIOKANDE collaboration, S. Fukuda et al., *Determination of solar neutrino oscillation parameters using 1496 days of super-kamiokande-i data*, *Phys. Lett.* **B 539** (2002) 179 [hep-ex/0205075];
 SNO collaboration, Q.R. Ahmad et al., *Measurement of day and night neutrino energy spectra at SNO and constraints on neutrino mixing parameters*, *Phys. Rev. Lett.* **89** (2002) 011302 [nucl-ex/0204009];
 SNO collaboration, B. Aharmim et al., *Electron energy spectra, fluxes and day-night asymmetries of B-8 solar neutrinos from the 391-day salt phase SNO data set*, *Phys. Rev.* **D 72** (2005) 055502 [nucl-ex/0502021].
- [2] SUPER-KAMIOKANDE collaboration, Y. Fukuda et al., *Evidence for oscillation of atmospheric neutrinos*, *Phys. Rev. Lett.* **81** (1998) 1562 [hep-ex/9807003].
- [3] SUPER-KAMIOKANDE collaboration, Y. Ashie et al., *A measurement of atmospheric neutrino oscillation parameters by Super-Kamiokande I*, *Phys. Rev.* **D 71** (2005) 112005 [hep-ex/0501064];
 SUPER-KAMIOKANDE collaboration, J. Hosaka et al., *Three flavor neutrino oscillation analysis of atmospheric neutrinos in Super-Kamiokande*, *Phys. Rev.* **D 74** (2006) 032002 [hep-ex/0604011].
- [4] KAMLAND collaboration, T. Araki et al., *Measurement of neutrino oscillation with KamLAND: evidence of spectral distortion*, *Phys. Rev. Lett.* **94** (2005) 081801 [hep-ex/0406035].
- [5] K2K collaboration, E. Aliu et al., *Evidence for muon neutrino oscillation in an accelerator-based experiment*, *Phys. Rev. Lett.* **94** (2005) 081802 [hep-ex/0411038].
- [6] MINOS collaboration, D.G. Michael et al., *Observation of muon neutrino disappearance with the MINOS detectors and the NuMI neutrino beam*, *Phys. Rev. Lett.* **97** (2006) 191801 [hep-ex/0607088].
- [7] OPERA collaboration, D. Autiero, *Status of the OPERA experiment (CNGS1)*, *Nucl. Phys.* **143** (Proc. Suppl.) (2005) 257;
 M. Guler et al., *Experiment proposal*, CERN/SPSC 2000-028 SPSC/P318 LNGS P25/2000.
- [8] G. Acquistapace et al., CERN-98-02.
- [9] LSND collaboration, A. Aguilar et al., *Evidence for neutrino oscillations from the observation of $\bar{\nu}/e$ appearance in a $\bar{\nu}_\mu$ beam*, *Phys. Rev.* **D 64** (2001) 112007 [hep-ex/0104049].
- [10] I. Stancu et al., FERMILAB-TM-2207.
- [11] G.L. Fogli, E. Lisi, A. Marrone and A. Palazzo, *Global analysis of three-flavor neutrino masses and mixings*, *Prog. Part. Nucl. Phys.* **57** (2006) 742 [hep-ph/0506083].
- [12] M. Maltoni, T. Schwetz, M.A. Tortola and J.W.F. Valle, *Status of global fits to neutrino oscillations*, *New J. Phys.* **6** (2004) 122 [hep-ph/0405172];
 T. Schwetz, *Neutrino oscillations: current status and prospects*, *Acta Phys. Polon.* **B36** (2005) 3203 [hep-ph/0510331].

- [13] B. Pontecorvo, *Mesonium and anti-mesonium*, *Sov. Phys. JETP* **6** (1957) 429 [*Zh. Eksp. Teor. Fiz.* **33** (1957) 549];
 Z. Maki, M. Nakagawa and S. Sakata, *Remarks on the unified model of elementary particles*, *Prog. Theor. Phys.* **28** (1962) 870;
 B. Pontecorvo, *Neutrino oscillation hypothesis*, *Sov. Phys. JETP* **26** (1968) 984 [*Zh. Eksp. Teor. Fiz.* **53** (1967) 1717];
 V.N. Gribov and B. Pontecorvo, *Neutrino astronomy and lepton charge*, *Phys. Lett.* **B 28** (1969) 493.
- [14] CHOOZ collaboration, M. Apollonio et al., *Limits on neutrino oscillations from the CHOOZ experiment*, *Phys. Lett.* **B 466** (1999) 415 [[hep-ex/9907037](#)];
 CHOOZ collaboration, M. Apollonio et al., *Search for neutrino oscillations on a long base-line at the CHOOZ nuclear power station*, *Eur. Phys. J.* **C 27** (2003) 331 [[hep-ex/0301017](#)].
- [15] K. Anderson et al., *White paper report on using nuclear reactors to search for a value of θ_{13}* , [hep-ex/0402041](#);
 F. Ardellier et al., *Letter of intent for double-CHOOZ: a search for the mixing angle θ_{13}* , [hep-ex/0405032](#).
- [16] Y. Itow et al., *The JHF-Kamioka neutrino project*, [hep-ex/0106019](#);
 T. Kobayashi, *Super beams*, *Nucl. Phys.* **143** (*Proc. Suppl.*) (2005) 303.
- [17] NOvA collaboration, D.S. Ayres et al., *NOvA proposal to build a 30-kiloton off-axis detector to study neutrino oscillations in the Fermilab numi beamline*, [hep-ex/0503053](#).
- [18] P. Huber, M. Lindner, T. Schwetz and W. Winter, *Reactor neutrino experiments compared to superbeams*, *Nucl. Phys.* **B 665** (2003) 487 [[hep-ph/0303232](#)];
 P. Huber, M. Lindner, M. Rolinec, T. Schwetz and W. Winter, *Prospects of accelerator and reactor neutrino oscillation experiments for the coming ten years*, *Phys. Rev.* **D 70** (2004) 073014 [[hep-ph/0403068](#)].
- [19] M.G. Albrow et al., *Physics at a Fermilab proton driver*, [hep-ex/0509019](#).
- [20] M. Baylac et al., *Conceptual design of the SPL II: a high-power superconducting H-linac at CERN*, CERN-2006-006.
- [21] M.V. Diwan et al., *Very long baseline neutrino oscillation experiments for precise measurements of mixing parameters and CP-violating effects*, *Phys. Rev.* **D 68** (2003) 012002 [[hep-ph/0303081](#)].
- [22] P. Zucchelli, *A novel concept for a $\bar{\nu}_e/\nu_e$ neutrino factory: the beta beam*, *Phys. Lett.* **B 532** (2002) 166.
- [23] NEUTRINO FACTORY/MUON COLLIDER collaboration, C. Albright et al., *The neutrino factory and Beta Beam experiments and development*, [physics/0411123](#).
- [24] A. Blondel et al., *ECFA/CERN studies of a European neutrino factory complex*, CERN-2004-002.
- [25] J.E. Campagne and A. Cazes, *The θ_{13} and $\delta(CP)$ sensitivities of the SPL-Fréjus project revisited*, *Eur. Phys. J.* **C 45** (2006) 643 [[hep-ex/0411062](#)].
- [26] M. Mezzetto, *Physics reach of the beta beam*, *J. Phys.* **G 29** (2003) 1771 [[hep-ex/0302007](#)];
 J. Bouchez, M. Lindroos and M. Mezzetto, *Beta beams: present design and expected performances*, *AIP Conf. Proc.* **721** (2004) 37 [[hep-ex/0310059](#)].

- [27] A. de Bellefon et al., *MEMPHYS: a large scale water Cerenkov detector at Frejus* [[hep-ex/0607026](#)].
- [28] C.K. Jung, *Feasibility of a next generation underground water Cherenkov detector: UNO*, *AIP Conf. Proc.* **533** (2000) 29 [[hep-ex/0005046](#)].
- [29] K. Nakamura, *Hyper-Kamiokande: a next generation water Cherenkov detector*, *Int. J. Mod. Phys. A* **18** (2003) 4053.
- [30] P. Huber, M. Maltoni and T. Schwetz, *Resolving parameter degeneracies in long-baseline experiments by atmospheric neutrino data*, *Phys. Rev. D* **71** (2005) 053006 [[hep-ph/0501037](#)].
- [31] P. Huber, M. Lindner and W. Winter, *Simulation of long-baseline neutrino oscillation experiments with globes*, *Comput. Phys. Commun.* **167** (2005) 195 [[hep-ph/0407333](#)].
- [32] P. Huber, M. Lindner and W. Winter, *Superbeams versus neutrino factories*, *Nucl. Phys. B* **645** (2002) 3 [[hep-ph/0204352](#)].
- [33] NUANCE event generator (v3), online at <http://nuint.ps.uci.edu/nuance>;
D. Casper, *The nuance neutrino physics simulation and the future*, *Nucl. Phys.* **112** (*Proc. Suppl.*) (2002) 161 [[hep-ph/0208030](#)].
- [34] M. Ishitsuka, T. Kajita, H. Minakata and H. Nunokawa, *Resolving neutrino mass hierarchy and CP degeneracy by two identical detectors with different baselines*, *Phys. Rev. D* **72** (2005) 033003 [[hep-ph/0504026](#)].
- [35] T. Kajita, H. Minakata, S. Nakayama and H. Nunokawa, *Resolving eight-fold neutrino parameter degeneracy by two identical detectors with different baselines*, *Phys. Rev. D* **75** (2007) 013006 [[hep-ph/0609286](#)].
- [36] K. Hagiwara, N. Okamura and K.-i. Senda, *Solving the neutrino parameter degeneracy by measuring the T2K off-axis beam in Korea*, *Phys. Lett. B* **637** (2006) 266 [[hep-ph/0504061](#)].
- [37] M. Mezzetto, *SPL and beta beams to the Fréjus*, *Nucl. Phys.* **149** (*Proc. Suppl.*) (2005) 179.
- [38] A. Donini, E. Fernandez-Martinez, P. Migliozi, S. Rigolin and L. Scotto Lavina, *Study of the eightfold degeneracy with a standard beta-beam and a super-beam facility*, *Nucl. Phys. B* **710** (2005) 402 [[hep-ph/0406132](#)].
- [39] J. Burguet-Castell, D. Casper, E. Couce, J.J. Gomez-Cadenas and P. Hernandez, *Optimal beta-beam at the CERN-SPS*, *Nucl. Phys. B* **725** (2005) 306 [[hep-ph/0503021](#)].
- [40] P. Huber, M. Lindner, M. Rolinec and W. Winter, *Physics and optimization of beta-beams: from low to very high gamma*, *Phys. Rev. D* **73** (2006) 053002 [[hep-ph/0506237](#)].
- [41] J. Burguet-Castell, D. Casper, J.J. Gomez-Cadenas, P. Hernandez and F. Sanchez, *Neutrino oscillation physics with a higher gamma beta- beam*, *Nucl. Phys. B* **695** (2004) 217 [[hep-ph/0312068](#)].
- [42] F. Terranova, A. Marotta, P. Migliozi and M. Spinetti, *High energy beta beams without massive detectors*, *Eur. Phys. J. C* **38** (2004) 69 [[hep-ph/0405081](#)].
- [43] M. Mezzetto, *Beta beams*, *Nucl. Phys.* **143** (*Proc. Suppl.*) (2005) 309 [[hep-ex/0410083](#)];
C. Volpe, *Topical review on 'beta-beams'*, *J. Phys. G* **34** (2007) 1 [[hep-ph/0605033](#)].
- [44] C. Volpe, *What about a beta beam facility for low energy neutrinos?*, *J. Phys. G* **30** (2004) 1 [[hep-ph/0303222](#)].

- [45] B. Autin et al., *The acceleration and storage of radioactive ions for a neutrino factory*, *J. Phys. G* **29** (2003) 1785 [physics/0306106];
M. Benedikt, S. Hancock and M. Lindroos, *Baseline design for a beta-beam neutrino factory*, proceedings of EPAC (2004), online at <http://accelconf.web.cern.ch/AccelConf/e04>;
M. Lindroos, EURISOL DS/TASK12/TN-05-02.
- [46] Eurisol Beta Beam webpage, <http://beta-beam.web.cern.ch/beta-beam>.
- [47] A. Blondel, M. Campanelli and M. Fechner, *Energy reconstruction in quasi-elastic events unfolding physics and detector effects*, *Nucl. Instrum. Meth. A* **535** (2004) 665.
- [48] M. Benedikt, A. Fabich, S. Hancock and M. Lindroos, *Optimization of the beta-beam baseline*, *Nucl. Phys.* **155** (Proc. Suppl.) (2006) 211.
- [49] M. Mezzetto, *Physics potential of the $\gamma = 100, 100$ beta beam*, *Nucl. Phys.* **155** (Proc. Suppl.) (2006) 214 [hep-ex/0511005].
- [50] The NEUGEN neutrino event generator, <http://minos.phy.tufts.edu/gallag/neugen>.
- [51] A. Fasso et al., Proceedings of the MonteCarlo 2000 conference, Lisbon, October 26 (2000), A. Kling et al. (eds.), Springer-Verlag Berlin (2001), pages 159 and 955.
- [52] Application Software group, Computing and Network Division et al., GEANT Description and Simulation Tool, CERN Geneva, Switzerland.
- [53] HARP collaboration, C. Catanesi et al., CERN-SPSC 2002/019;
MINERVA collaboration, D. Drakoulakos et al., *Proposal to perform a high-statistics neutrino scattering experiment using a fine-grained detector in the NuMI beam*, hep-ex/0405002.
- [54] M. Mezzetto, *Physics potential of the SPL super beam*, *J. Phys. G* **29** (2003) 1781 [hep-ex/0302005].
- [55] M. Honda, T. Kajita, K. Kasahara and S. Midorikawa, *A new calculation of the atmospheric neutrino flux in a 3-dimensional scheme*, *Phys. Rev. D* **70** (2004) 043008 [astro-ph/0404457].
- [56] P. Lipari and T. Stanev, *Propagation of multi-TeV muons*, *Phys. Rev. D* **44** (1991) 3543.
- [57] M.C. Gonzalez-Garcia and M. Maltoni, *Atmospheric neutrino oscillations and new physics*, *Phys. Rev. D* **70** (2004) 033010 [hep-ph/0404085].
- [58] J. Burguet-Castell, M.B. Gavela, J.J. Gomez-Cadenas, P. Hernandez and O. Mena, *On the measurement of leptonic CP-violation*, *Nucl. Phys. B* **608** (2001) 301 [hep-ph/0103258].
- [59] H. Minakata and H. Nunokawa, *Exploring neutrino mixing with low energy superbeams*, *JHEP* **10** (2001) 001 [hep-ph/0108085].
- [60] G.L. Fogli and E. Lisi, *Tests of three-flavor mixing in long-baseline neutrino oscillation experiments*, *Phys. Rev. D* **54** (1996) 3667 [hep-ph/9604415].
- [61] V. Barger, D. Marfatia and K. Whisnant, *Breaking eight-fold degeneracies in neutrino CP-violation, mixing and mass hierarchy*, *Phys. Rev. D* **65** (2002) 073023 [hep-ph/0112119].
- [62] O. Yasuda, *New plots and parameter degeneracies in neutrino oscillations*, *New J. Phys.* **6** (2004) 83 [hep-ph/0405005].
- [63] S. Antusch, P. Huber, J. Kersten, T. Schwetz and W. Winter, *Is there maximal mixing in the lepton sector?*, *Phys. Rev. D* **70** (2004) 097302 [hep-ph/0404268].

- [64] H. Minakata, M. Sonoyama and H. Sugiyama, *Determination of θ_{23} in long-baseline neutrino oscillation experiments with three-flavor mixing effects*, *Phys. Rev. D* **70** (2004) 113012 [[hep-ph/0406073](#)].
- [65] A. Donini, E. Fernandez-Martinez, D. Meloni and S. Rigolin, *ν_μ disappearance at the SPL, T2K-I, NO ν A and the neutrino factory*, *Nucl. Phys. B* **743** (2006) 41 [[hep-ph/0512038](#)].
- [66] O.L.G. Peres and A.Y. Smirnov, *Atmospheric neutrinos: LMA oscillations, $U(e3)$ induced interference and CP-violation*, *Nucl. Phys. B* **680** (2004) 479 [[hep-ph/0309312](#)].
- [67] M.C. Gonzalez-Garcia, M. Maltoni and A.Y. Smirnov, *Measuring the deviation of the 2-3 lepton mixing from maximal with atmospheric neutrinos*, *Phys. Rev. D* **70** (2004) 093005 [[hep-ph/0408170](#)].
- [68] S.T. Petcov, *Diffraction-like (or parametric-resonance-like?) enhancement of the Earth (day-night) effect for solar neutrinos crossing the Earth core*, *Phys. Lett. B* **434** (1998) 321 [[hep-ph/9805262](#)];
M. Chizhov, M. Maris and S.T. Petcov, *On the oscillation length resonance in the transitions of solar and atmospheric neutrinos crossing the Earth core*, [hep-ph/9810501](#);
M.V. Chizhov and S.T. Petcov, *New conditions for a total neutrino conversion in a medium*, *Phys. Rev. Lett.* **83** (1999) 1096 [[hep-ph/9903399](#)].
- [69] E.K. Akhmedov, *Parametric resonance of neutrino oscillations and passage of solar and atmospheric neutrinos through the Earth*, *Nucl. Phys. B* **538** (1999) 25 [[hep-ph/9805272](#)];
E.K. Akhmedov, A. Dighe, P. Lipari and A.Y. Smirnov, *Atmospheric neutrinos at super-Kamiokande and parametric resonance in neutrino oscillations*, *Nucl. Phys. B* **542** (1999) 3 [[hep-ph/9808270](#)].
- [70] J. Bernabeu, S. Palomares Ruiz and S.T. Petcov, *Atmospheric neutrino oscillations, θ_{13} and neutrino mass hierarchy*, *Nucl. Phys. B* **669** (2003) 255 [[hep-ph/0305152](#)].
- [71] C.W. Kim and U.W. Lee, *Comment on the possible electron-neutrino excess in the super-Kamiokande atmospheric neutrino experiment*, *Phys. Lett. B* **444** (1998) 204 [[hep-ph/9809491](#)].
- [72] T. Kajita, Talk at NNN05, 7–9 April 2005, Aussois, Savoie, France, <http://nnn05.in2p3.fr>.
- [73] S.T. Petcov and T. Schwetz, *Determining the neutrino mass hierarchy with atmospheric neutrinos*, *Nucl. Phys. B* **740** (2006) 1 [[hep-ph/0511277](#)].
- [74] O. Mena Requejo, S. Palomares-Ruiz and S. Pascoli, *Super-NO ν A: a long-baseline neutrino experiment with two off-axis detectors*, *Phys. Rev. D* **72** (2005) 053002 [[hep-ph/0504015](#)];
O. Mena, S. Palomares-Ruiz and S. Pascoli, *Determining the neutrino mass hierarchy and CP-violation in NO ν A with a second off-axis detector*, *Phys. Rev. D* **73** (2006) 073007 [[hep-ph/0510182](#)].
- [75] V. Barger et al., *Precision physics with a wide band super neutrino beam*, *Phys. Rev. D* **74** (2006) 073004 [[hep-ph/0607177](#)].
- [76] M. Kachelriess and R. Tomas, *Identifying the neutrino mass hierarchy with supernova neutrinos*, [hep-ph/0412100](#).
- [77] Webpage of the International Scoping Study physics working group:
<http://www.hep.ph.ic.ac.uk/iss/wg1-phys-phen/index.html>.

Erratum

The correct address of the Instituto de Física Teórica is:

*Instituto de Física Teórica UAM-CSIC, Facultad de Ciencias C-XVI,
Universidad Autónoma de Madrid, Cantoblanco, Madrid 28049, Spain*

JHEP04(2007)003